RADIATION DAMAGE IN MAGNESIUM FLUORIDE

By

CLAUDE DONALD NORMAN

Bachelor of Science
Berry College
Mt. Berry, Georgia
1958

Master of Science
University of Georgia
Athens, Georgia
1967

Submitted to the Faculty of the Graduate College
of the Oklahoma State University
in partial fulfillment of the requirements
for the Degree of
DOCTOR OF PHILOSOPHY
July, 1976

RADIATION DAMAGE IN MAGNESIUM FLUORIDE

Thesis Approved:

Larry E. Halliburton
Thesis Adviser

W. A. Sibley

George S. Dick

Joel J. Martin

J. Paul Gerlich

Norman N. Durham
Dean of the Graduate College

ACKNOWLEDGEMENTS

The author wishes to express his deepest appreciation to Larry Halliburton, friend and thesis advisor. Without his patience, encouragement, and 'total' dedication this work would have certainly fallen short of its goal. The author also wishes to extend a special thanks to other members of the ESR group; Gene Little, Mark Young and K. Saha.

Completion of this work represents the continuous support of a number of professional people. The initial desire was planted by Dr. 'Mac' (Berry College), cultivated by the physics faculty of two universities and scores of friends. A special thanks is due my parents. It was their stimulating lives that initiated the early steps of this journey. Finally, to my wife and children, who made the long and hard journey worthy of travel. To all of you, I am grateful.

The author graciously acknowledges the financial support of the National Science Foundation and the Physics Department at Oklahoma State University.

TABLE OF CONTENTS

TABLE OF CONTENTS (Continued)

LIST OF TABLES

LIST OF FIGURES

CHAPTER I

RADIATION DAMAGE

Introduction

Long before a given material joins the 'useful' category, it is normally subjected to a fundamental research program. Electrical, mechanical, optical, thermal, and magnetic properties are measured in hopes of completely characterizing the material. Often, many different experimental tools are used for these measurements. Color center physics (1) constitutes just one of these areas of fundamental research.

Within the last two decades, important progress in determining the 'structure of defects' has been partially due to the new methods of paramagnetic resonance; ESR (Electron Spin Resonance (2)) and ENDOR (Electron Nuclear Double Resonance (3)). These methods have provided the power of an ultrasensitive microscope for color center research. Through the hyperfine interaction, these methods are capable of presenting a very detailed picture of the center and its surroundings; a picture with many points and with high information capacity. ESR and ENDOR provide information about the ground state electronic structure of paramagnetic centers with a depth and accuracy unattainable by other methods.

Alkali Halide Crystals

Because of their many favorable properties (strongly ionic, rare-

gas electronic configuration, width of valence band, mechanical, and growth properties), the alkali halide crystals have been the subject of considerable color center research (4) aimed at understanding the effect of ionizing radiation on the solid state.

These crystals have been subjected to different types of radiation (electrons, protons, neutrons, X-rays, gamma-rays and ultraviolet photons) over a wide range of temperatures. Detectable radiation damage in the form of isolated, as well as clustered, vacancies and interstitials produced by the displacement of ions from their normal sites have been observed by both optical and ESR techniques.

The most frequently studied of these point defects has been the F center (a negative ion vacancy which has trapped an electron) (5). Despite intensive study of the F center for many years, no definitive radiation-damage mechanism emerged. One of the major problems consisted of explaining how incoming photons (x-rays, γ-rays) could displace negative ions when they lacked sufficient momentum for a direct collision process. Within the past twenty years various proposals to explain this behavior, all based on initial ionziation events, have been made and will be examined in the next section.

Defect Models

When alkali halide crystals are irradiated with electrons, or even ultraviolet light in some cases, many ionic defects (6) are produced. Experimentally, in these ionic materials defect creation is highly efficient and most likely due to conversion of electronic energy into a form capable of creating lattice defects. This suggests an ionization of the halogen ion.

The first of these production mechanisms was proposed by Varley (7). He suggested that if a negative halogen ion was doubly ionized, thus turning it into a positive ion, and if this charge state could exist for several lattice vibrations, the ion would be displaced from its lattice site and yield the observed Frenkel pair (interstitial-vacancy pair). The two electrons removed in the initial ionization could be captured by both the vacancy and the interstitial giving the F center and H center (an interstitial atom center). Work by several research groups (8,9,10) considered the problematic lifetime of a doubly ionized state. They concluded that it was not possible to exclude the double ionization mechanism as a prerequisite for radiation damage, but that it was an unlikely event.

Another mechanism in which both isolated double ionizations and correlated single ionizations would give rise to F centers and H centers was proposed by Klick (11). He considered the formation of a neutral halogen molecule as the end product of either type of ionization.

Howard (12) was the first to introduce a model which did not invoke a diffusion type process to satisfactorily account for the experimentally observed separation of F and H centers. In his model the interaction was between a doubly ionized halogen and a neighboring ion.

Using a Born-Mayer potential, Balarin (13) fabricated a direct displacement (via elastic electron-ion collisions) [110] focusing model. He concluded that photoelectrons generated through X-ray absorption processes could possibly but not probably produce interstitials.

Many of the previous models require two ionizing events to occur on nearest neighbor sites on the anion lattice. However, since correlated double ionization events are low in probability, many workers in

the field believed that only a single ionization event was involved in the mechanism. A more complete review will now be given of a single ionization mechanism (Pooley-Hersh) which appears to satisfy all the experimental observations concerning the radiation damage process at low temperatures in halide materials.

Pooley-Hersh Production Mechanism

Studies of ultraviolet irradiation and corresponding luminescence in potassium iodide by several research groups (14,15) opened the doors to our most successful damage mechanism. Hersh (16) noted that while the ionizing radiation was on, the most pronounced phenomenon at low temperature was a characteristic luminescence; after the radiation is turned off, only the stable defects remain. The Pooley-Hersh mechanism (17), as frequently and properly named, proposes that during irradiation there exist within the crystal a high density of excitonic molecules (bound electron-hole pairs). Some of these excitons luminesce, others decay by emission of phonons, while still others decay by a mode leading to F center-H center production. In this latter mode, the energy stored in the lattice surrounding the excitonic molecule (or V_K center) is sufficient to start a replacement sequence (18) which results in a reasonable separation of the interstitial from the vacancy.

This defect mechanism, based on electron-hole recombination, is supported by the experimentally (19,20) observed fact that in KI the yield of F centers increases abruptly in the same temperature range where there is a drastic loss in luminescence efficiency. Correlation between F center production and fundamental luminescence has been observed in other materials (21), RbI and NaI for example; however, recent

investigations have shown that this correlation does not exist in all halide materials. Finally, accumulated experiments on a variety of alkali halide materials strongly suggest that low temperature irradiation introduces empty anion vacancies and interstitial halide ions as well as F and H centers, but that the former do not persist to very high temperatures (1).

Once the basic premises of the Pooley-Hersh mechanism are accepted, the next question is whether the isolated vacancy exist briefly with subsequent trapping of an electron or whether the F center is formed instantaneously. Konitzer and Hersh (15) have suggested that the Frenkel pair separates by diffusion of the atomic halogen atom. Lushchik (22) favors the direct production of F center-interstitial atom pairs rather than the empty vacancy-interstitial ion pairs suggested by Pooley. Recent experiments by Itoh (23) suggest that the empty vacancy may never appear as a separate entity.

Focusing

Clearly, the interstitial must move a few lattice spaces from the vacancy upon creation. Pooley has suggested a [110] replacement sequence (18) for the alkali halides. Using a computer simulated [110] replacement sequence, Pooley has obtained 4-5 ev replacement thresholds in many of the alkali halides. If the electron-hole recombination energy is not equally shared, it is postulated that the more energetic ion may move at least several lattice spaces from the F center site in a [110] direction. At low temperatures the exact nature of the Frenkel pair resulting from this process seems to depend upon the magnitude of the Coulomb and elastic interactions between the vacancy and the inter-

stitial and hence their final separation.

V_K Center

Trapped-hole centers (24) have played and continue to play a very important role in the development of our understanding of radiation damage behavior. Despite extensive studies in select materials, these centers are still poorly understood. The principle aim of this dissertation is to expand our knowledge of self-trapped hole centers (V_K) in a non-focusing material.

Structure

An electron is removed from a halide lattice ion in an ionization event, leaving behind a hole. The resulting halide atom then combines with a nearest-neighbor [110] halide ion. This leads to distortion in the surrounding lattice and thus creates a potential well in which the hole becomes 'self-trapped'. The hole is equally shared in a covalent bond between the two halides. Thus, the molecular-ion character is established.

The intrinsic V_K spectrum is independent of impurities and for the most part does not change substantially with the cation. That is, there is only a very weak interaction between the V_K center and the surrounding lattice. It is the electronic structure of the material, not the ionic structure, which is altered by this defect.

The V_K center is paramagnetic and to a good approximation axially symmetric. Daly and Mieher (25) have shown the center to be intrinsic in the sense that no other defects such as vacancies or interstitials are involved.

Production

In order that a V_K center be produced the accompanying electron must be trapped at some other defect, such as an impurity. The production rate is found to be extremely dependent on the number of electron traps. Within the temperature range of 100-200 K, in most materials, the center irreversibly disappears as a result of hole mobility and subsequent electron-hole recombination. Unless the material is deliberately doped with some electron-trapping impurity, electron-hole recombination severely limits V_K center concentration. For example, the production rate for KCl:Tl is about 10^{+3} times larger than pure KCl for a given irradiation (24). Since V_K formation is a simple ionization process for all materials reported in the literature, their production is quite efficient and tends to saturate rapidly with dose.

Decay

The V_K center is a very effective electron trap. During irradiation a substantial fraction of the electron-hole pairs produced will recombine immediately. Excitation energy released by the decay process may appear as luminescence, phonon production, Frenkel pair production, or excitation energy in existing defects. The particular mode will depend upon temperature, host lattice and impurity concentration. Color center researchers believe the V_K center production mode to be the heart of the previously mentioned Pooley-Hersh damage mechanism. A novel aspect of this mechanism is that the death of a V_K center could and often does become the birth of yet other defects-the F center and H center (split interstitial atom).

Orientation

The low symmetry of the V_K center (in all cases axial) may be utilized to extend our understanding of these defects. Studies of V_K center orientation, through polarized or dichroic absorption, were first carried out by the Argonne group (26,27).

In the case of the cubic NaCl structure, V_K centers will be distributed uniformly among the six [110] directions. Certain orientations can be preferentially populated through polarized bleaching. Keller and Murray (28) observed the fundamental luminescence associated with electron-hole recombination at previously aligned V_K centers. This luminescence reflected the orientation of the V_K center before electron capture.

Mobility

Considerable work has been done on the motion of the intrinsic V_K centers and their interaction with impurity ions (29). Above a certain temperature, depending upon the material, V_K centers can move through the lattice. This effect has been studied in several systems by observing "glow peaks"(thermoluminescence bands) that occur when a V_K center recombines with an electron. In KCl, the mobility of the V_K center becomes detectable at about 170 K (27) whereas in LiF, KBr and KI the corresponding temperatures are 110, 140 and 90 K respectively (26,28). Keller and Murray (28), while monitoring the decrease of the V_K band and concomitant recombination luminescence, concluded that hopping by discrete reorientation steps is the dominant mechanism for V_K center motion. Translation and reorientation are thus aspects of the same process.

V_{KA} Center

In this center (30) one of the nearest-neighbor lattice sites of the V_K center is occupied by an impurity ion or other lattice defect. These centers are generally produced in doped crystals by first irradiating at a low temperature, creating the intrinsic V_K, then annealing above a temperature at which the V_K is mobile. The V_{KA} center is formed when the intrinsic V_K encounters an impurity and becomes trapped.

The V_K and V_{KA} center spectra are nearly indistinguishable. Differentiation between centers is usually accomplished through thermal anneal studies.

H Center

The intrinsic interstitial defect is one of the most fundamental of defects in solids. Direct characterization of this center by Känzig and Woodruff (31) in KCl, KBr and LiF represented the first detailed interstitial color center work. Contrary to expectation, the interstitial has never been observed as a single atom in the halides. In all known cases the interstitial halide atom combines with a substitutional lattice ion to form a molecule-ion centered on a single lattice site. There is a small but measureable overlap of the hole onto the two additional halide ions located at each end of the molecular ion.

The H center is usually produced at extremely low temperature and often exhibits motional effects. In contrast to the V_K center, reorientation does not necessarily imply translation for H centers (32).

Keller-Patten Experiment

Today this experiment (33) offers the most convincing proof of the

Pooley-Hersh damage mechanism. Basically the experiment reveals how H centers are created by destroying V_K centers. Briefly, V_K centers were created by electron irradiation at 77 K. Cooling to helium temperatures, the crystal was bleached with IR light. This released electrons which recombined with holes (V_K centers) and led to production of F and H centers. According to the Pooley-Hersh mechanism the number of interstitials formed as a result of the IR light was found to be in direct proportion to the number of V_K centers destroyed.

CHAPTER II

ELECTRON SPIN RESONANCE

Introduction

The principles of ESR and the information obtained by this technique have been presented in a number of books (34,35,36) and review articles (37,38,39) with which this chapter does not attempt to compete. In this chapter, only the theory of ESR as applicable to color centers will be considered. Before launching our discussion, consider the following spin Hamiltonian (37):

$$\begin{aligned} \mathcal{H} = {} & \beta(g_x H_x S_x + g_y H_y S_y + g_z H_z S_z) + D\left[S_z^2 - \frac{1}{3}(S)(S+1)\right] + E(S_x^2 - S_y^2) \\ & + A_x S_x I_x + A_y S_y I_y + A_z S_z I_z + F\left[I_z^2 - \frac{1}{3}(I)(I+1)\right] \\ & + F'(I_x^2 - I_y^2) - g_N \beta_N \vec{H}\cdot\vec{I} \end{aligned} \tag{1}$$

where H - magnetic field, S - effective electron spin, I - nuclear spin, g - spectroscopic splitting tensor, D and E - zero-field splitting parameters, A - hyperfine splitting parameters, F and F' - nuclear quadrupole splitting parameters, and g_N - nuclear g factor. To the ESR experimentalist, this equation represents the cross roads of 'experiment' and 'theory'. For this chapter it serves as an outline. Only select topics aimed at a physical understanding of this equation will be pre-

sented in this chapter.

Magnetic Resonance

Magnetic resonance, a fundamental branch of spectroscopy, has been a valuable addition to the methods of investigating point defects in solids. The technique is regarded as complementary to optical investigations.

Each configuration of unpaired electrons exhibits a characteristic spectrum (40). Detailed information is provided about the local environment of the magnetic defects. The ESR spectra are very sensitive to site symmetry and small departures from the normal structure. Thus, the method provides detailed information concerning the structure of color centers which could not be obtained from optical techniques. In the alkali halide crystals, interaction with magnetic moments of both halogen and alkali nuclei have allowed detailed electronic wave functions (5) to be determined in several cases (F, H and V_K centers). Defect concentration, nuclear spin, relaxation times, g-factors and other parameters have been measured by this powerful technique.

Crystal Field

When the term paramagnetic resonance is used, one frequently thinks of a loosely coupled system (free ion system). For example, gas or liquid substances where each permanent magnetic dipole is essentially independent of its neighbors. Such free ion systems have a resultant angular momentum due partly to the orbital motion and partly to the intrinsic spin of the electrons.

In the solid state the electrons are subjected to enormous elec-

tric fields from the surrounding atoms. Imagine the paramagnetic ion at a normal lattice site, surrounded by a regular array of diamagnetic ions. Here it is assumed that the influence of the neighboring ions occurs entirely through the electric field they produce at the paramagnetic ion site. These unpaired electrons experience forces due to this field which modify their usual orbital motion. For example, in the 3d iron group, this interaction is so great that the orbital momentum of the electron is almost completely quenched; that is, the orbits are locked into the crystalline electric field and are uninfluenced by any external magnetic field which we can produce. Orbital motion cannot make its proper contribution to the magnetism. Electron spin and its associated magnetic moment has no direct interaction with the electrostatic field and is free to orient itself in the external magnetic field, the only external constraint being the spin-orbit coupling. In summary, for the 3d iron group, the crystal field interaction is stronger than spin-orbit coupling, and the effective g-factor approaches the free spin value.

The electric field produced at the magnetic ion site may be considerably reduced by screening. In the case of the rare earth ions, the unpaired electrons are in the 4f shell and screened by 5s and 5p electrons. Both orbital and spin associated magnetic moments make a contribution to magnetism. When the orbital motion is only partially quenched, the orbital magnetic moment is appreciable and large magnetic anistropy exists.

g-Tensor

This spectroscopic splitting factor (41) is analogous to the Lande'

splitting factor for a free ion, but in general has different values for an ion in a crystal. This is due to the crystalline electric field and its ability to modify orbital magnetic moments.

The magnitude of the orbital contribution to the magnetic moment depends on the crystal field. It's magnitude is usually different for different directions of the external magnetic field H, thus showing an angular variation which follows the symmetry of the crystal field. (In practice the crystal field symmetry is determined largely by nearest neighbor ions.) The total g-value may then be anisotropic by an amount which depends on the magnitude of the orbital contribution to the magnetic moment, and the asymmetry in the crystal field. For all cases, an anisotropic g-value can be represented by a second-rank tensor; it expresses the admixture of close lying excited states into the 'ground' state via the spin-orbit interaction. In practice this tensor appears in the electronic Zeeman term of the spin Hamiltonian (42).

Hyperfine Interaction

If any nuclei in the vicinity of the unpaired electrons have a magnetic moment, they will interact with the electronic magnetic moment and result in hyperfine structure (hfs) in the ESR spectra. A simple manner of regarding the origin of hfs is to think of the nuclear moment as producing a magnetic field which interacts with the electronic magnetic moment. This additional field, up to a few hundred gauss normally, is added to the external field. The magnitude of this effective field depends on the magnetic quantum state of the nucleus which is assumed fixed during an electronic transition. Since there are 2I+1 possible values for the nuclear magnetic quantum number, there will be

2I+1 effective magnetic fields with which the electronic magnetic moment can interact. As a result, the resonance line will split into 2I+1 hyperfine components. Allowed ESR transitions are those for which $\Delta m_I = 0$ and $\Delta m_S = \pm 1$. Hyperfine lines are of equal intensity and are equally spaced. This spacing normally varies with different directions of H. The hyperfine structure spacing can be described by the principal values of the hyperfine tensor, A_x, A_y and A_z.

Line Widths

Any interaction between the magnetic ion and its surroundings will possibly broaden the lines. Line broaden can be classified as homogeneous or inhomogeneous. Homogeneous broadening occurs when the spin lifetime becomes very short and is a direct result of the uncertainty principle. Inhomogeneous broadening is a result of unresolved hyperfine interactions.

Spin Hamiltonian

In the preceeding sections, the various terms appearing in Equation (1) have been identified. The problem facing the ESR spectroscopist is to determine values for the spin operator coefficients appearing in the spin Hamiltonian. Since this is the usual eigenvalue problem, one normally proceeds to express the spin Hamiltonian in matrix form by expanding it in the spin manifold appropriate to the problem. Computer diagonalization is then used to determine the energy eigenvalues for a given set of values for the parameters. By systematically varying the parameter values, one can obtain a best-fit to the experimental line positions.

CHAPTER III

PURPOSE OF THIS INVESTIGATION

Introduction

Radiation damage effects in the alkali halide crystals have been the subject of numerous and fruitful investigations. However, until recently, there was very little work done outside the alkali halide crystals. The research reported in this dissertation represents part of a continuing effort of a small number of researchers to expand our present knowledge of radiation damage to more complicated materials; for example, the rutile structured materials. These materials should provide new testing grounds for the various damage mechanisms previously discussed.

Rutile Structure

The rutile crystal structure is based on a tetragonal unit cell. Figure 1 shows two unit cells of MgF_2; each cation (Mg^{++}) is surrounded by a distorted octahedron of six anions (F^-), with four nearest neighbors at a distance of 1.89Å and two at 1.994Å (43). There are two distorted octahedra which are equivalent except for a 90^o rotation about the tetragonal or c-axis of the unit cell (see Figure 2).

Previous Work in MgF_2

A literature search of color centers in any one of the alkali

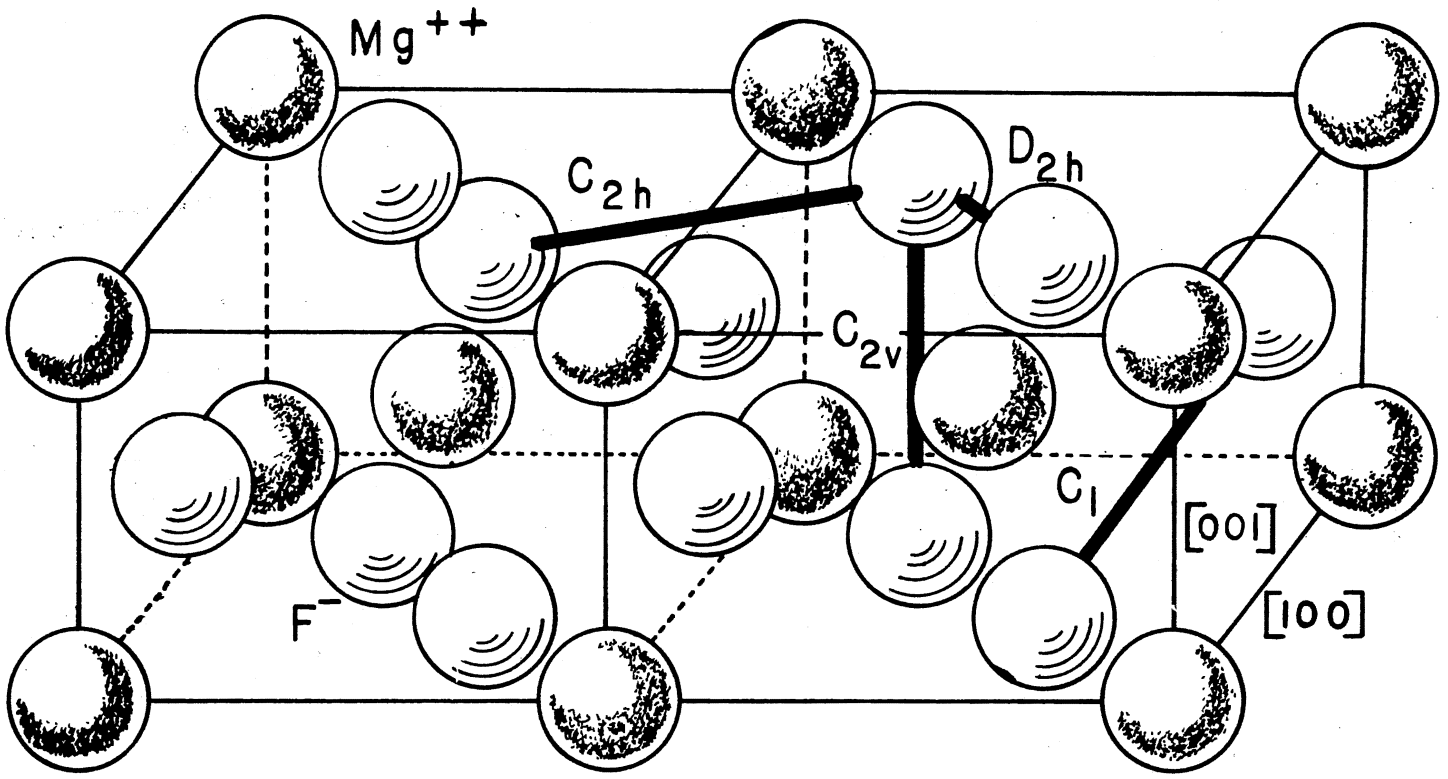

Figure 1. Two Conventional Unit Cells for the Rutile Structured MgF_2

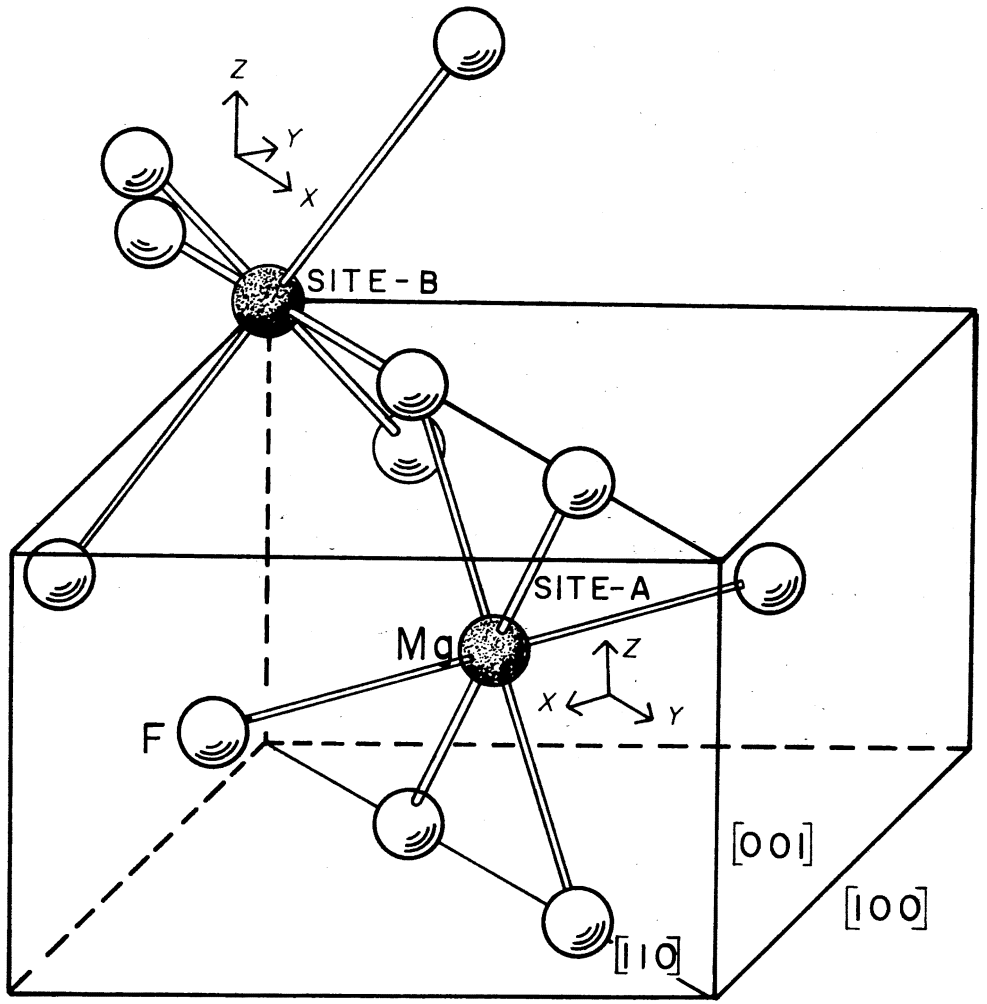

Figure 2. Diagrammatic Representation of the Two Non-equivalent Cation Sites in the MgF_2 Structure

halide materials will provide an enormous volume of reading material. By comparison, few color center investigations exist for MgF_2 crystals. Although leaning heavily upon the shoulders of the alkali halide work, the following summaries represent the present 'state of the art' for color centers in MgF_2.

Duncanson and Stevenson

While this work (44) mostly addressed the physical properties (density, melting point, lattice constants) of MgF_2, the authors reported the appearance of a u.v. absorption band (1100-1360Å) after X-irradiation.

Hills and McBride

Hills and McBride reported (45) briefly on an optical study of MgF_2 irradiated at room temperature. They suggested an assignment of the bands near 260 nm and 370 nm to the conventional F and M centers, respectively.

Blunt and Cohen

Color centers were produced (46) by 50-KeV X-rays at room temperature. Optical absorption and optical preferential bleaching studies were made on several oriented single crystals. On the basis of group theoretical arguments, the strong 260 nm absorption band was assigned to the F center. Bands at 370 and 320 nm were believed due to the M center.

Sibley and Facey

At last, an in-depth color center study was made on a rutile structured material (47). Production, (sample, temperature, and irradiation intensity dependence), optical absorption, and thermal decay were all investigated and compared with alkali halide results. The conclusion was that the Pooley-Hersh damage mechanism was operative and because no focusing directions exist, correlated Frenkel pairs were created at low temperature (48).

Facey, Lewis and Sibley

A comparison of electron and neutron irradiated MgF_2 crystals was made under carefully controlled conditions. The conclusion (49), not too surprising, was that neutron irradiated crystals contain more cluster defects than electron irradiated crystals.

Unruh, Nelson, Lewis and Kolopus

The F center was absolutely identified in electron irradiated MgF_2 by using the ENDOR technique (50). Samples were irradiated at both room temperature and 77K. In a companion paper, these same authors correlated the optical and ESR signals of the F center. They also reinforced the results of Sibley and Facey concerning the minimum in colorability of MgF_2 at 150K. Their investigation produced only one ESR spectrum, that of the F-center, even though irradiations were performed at 77K.

Buckton and Pooley

In order to explain the unusual F center production, that is, sig-

nificant F center production at low and high temperature and nearly zero production at intermediate temperature (100-200 K), a F center-H center close pair model was proposed (51). Once created, the F-H close pair remains stable, recombines, or dissociates according to the temperature. Evidence for the existence of such a pair was provided by measuring the F center optical line width for samples irradiated at 5K and 300K. Bands produced at 5K and measured at 5K were broader than the corresponding band produced at 300K and measured at 5K.

Summary

The purpose of this investigation is to extend our present knowledge of radiation damage to a non-focusing rutile structured material. In analogy with the alkali halides, the self-trapped hole center is expected to play an important role in the damage process. While sufficient evidence has been presented to substantiate the Pooley-Hersh mechanism in MgF_2, the self-trapped hole center has not been observed. Our specific objective in this dissertation is to create, stabilize, and measure the ESR parameters describing the self-trapped hole centers in MgF_2 and possibly provide further evidence to test the validity of the proposed F-H center close pair theory.

CHAPTER IV

EXPERIMENTAL APPARATUS AND PROCEDURE

Introduction

Since its discovery in 1945, the techniques of ESR spectroscopy have touched upon many disciplines, each with its own unique problem and each with its own talent to improve upon whatever system it inherited. Basically, the instrumentation and techniques employed in this research are the same as that reported by Rhoads (52). Rather than duplicate specific instrument descriptions, the following paragraphs will enlarge upon modifications made during the course of this investigation. Hopefully, the basic system was improved.

Crystals

Crystals used during this investigation were obtained from two different sources. W. A. Sibley supplied what appears to be the 'purest' crystals. These were single crystals obtained from the Harshaw Chemical Company. In fact, these crystals came from the same ingot as used by Sibley-Facey (1968) and Unruh et al. (1971). A list of impurity concentrations determined through neutron activation, mass-spectrographic analysis, and flame-absorption spectroscopy has been reported (47). Other crystals that were examined during this experiment came from the Crystal Growth Laboratory of this University. These were random crystal cuttings (Harshaw) used as a starting material in our $KMgF_3$ program.

Although no formal impurity analysis was made, our ESR spectra indicated a higher impurity concentration for these samples.

One of the major difficulties encountered was that of orienting our samples to provide mounting planes for angular studies. Since MgF_2 does not readily cleave, crystallographic axes for all samples were determined by taking a series of back-reflection Laue patterns. In practice, the exact orientations of the crystals were obtained in the ESR spectrometer by minimizing the width of those ESR lines that split most rapidly for small angular variation.

Once approximately oriented by the Laue technique, samples were cut with a diamond saw to sizes convenient for our dewar systems. The nitrogen finger dewar system, used with the Varian V-4531 rectangular cavity, is shown in Figure 3. The size of the inner tube, 5 mm I.D., severely limits the size of samples utilized in our 77K studies. Sample sizes for the helium dewar system shown in Figure 4 were also limited; the limiting factor being the shift in cavity frequency. Very large samples shifted the cavity frequency outside the range of the microwave klystron. These constraints limited our samples to those reported in Table I.

Irradiation of Samples

During the early stages of this experiment, samples were mounted on the end of a copper rod with silicon high vacuum grease then irradiated at 77K inside a styrofoam cup (previously explained by Rhoads). A problem with this technique was that irradiated silicon grease develops an enormous ESR signal in the $g \approx 2$ region-thus eliminating this crucial region of the ESR spectra. To eliminate this problem, the sample holder of Figure 3 was implemented. Now samples could be electron irradiated

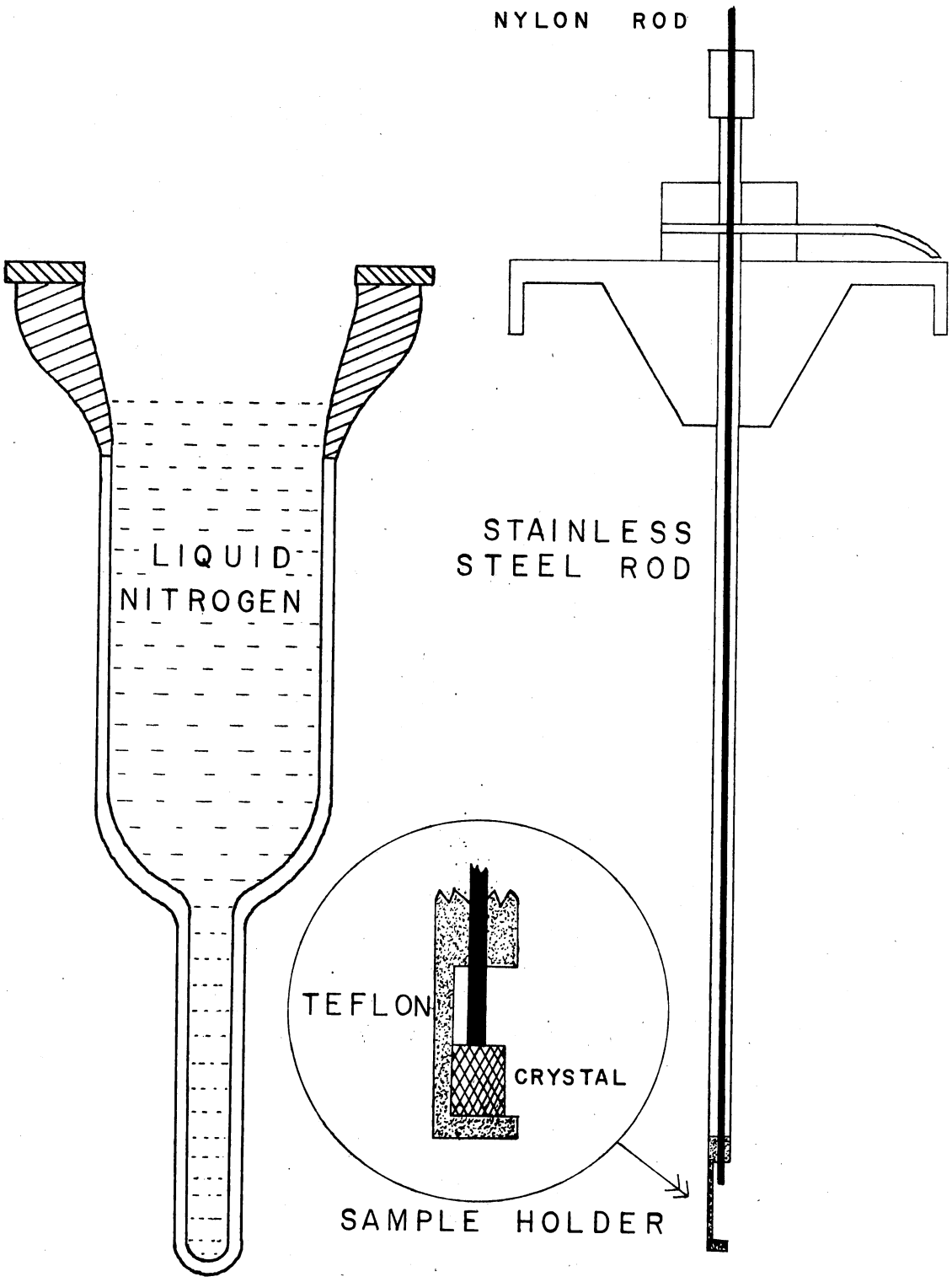

Figure 3. (a) Glass Finger Dewar System (77K);
(b) Sample Holder

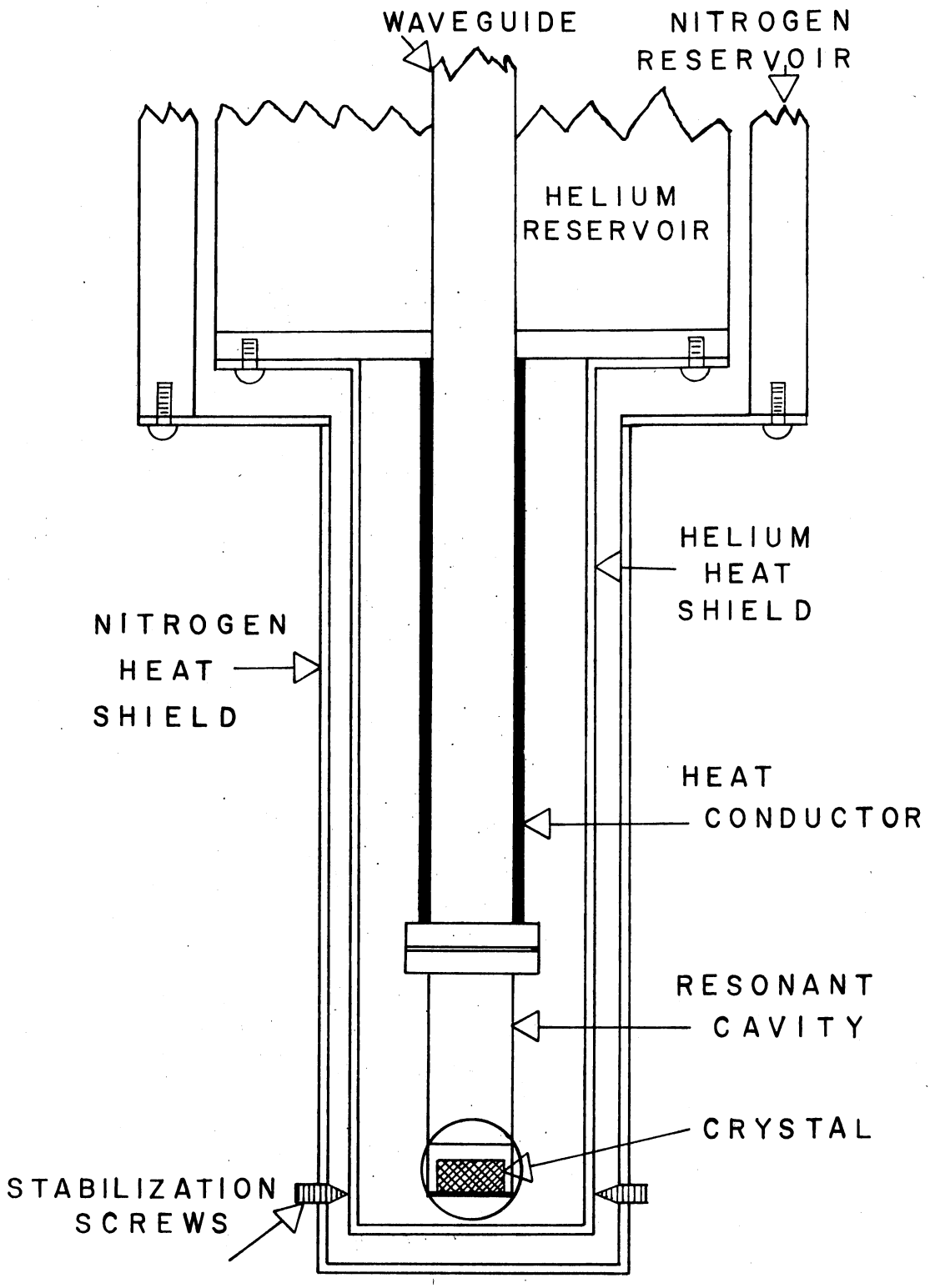

Figure 4. Helium Dewar System (5K)

TABLE I

SAMPLE CHARACTERISTICS

Sample	Size (mm)	Mass (gm)	Mounting Plane	Dewar System	Possible Field Directions (90^{o} Rotation)
Al (optical)	1.1 x 3.2 x 7.5	0.078	(010)	Nitrogen	[100] to [001]
A	2.5 x 3.2 x 5.1	0.121	(010)	Nitrogen	[100] to [001]
C	2.3 x 3.2 x 7.8	0.181	$(\bar{1}10)$	Nitrogen	[110] to [001]
E	2.6 x 3.5 x 11.0	0.334	(001)	Nitrogen	[100] to [010]
F	2.5 x 3.7 x 11.0	0.320	$(\bar{1}10)$	Helium	[110] to [001]

at 77K without interference from the broad grease line.

Irradiations at 5K were done, as described by Rhoads, in a stainless steel dewar using silicon grease to secure the sample on the bottom plate of the TE_{102} rectangular cavity (see Figure 4).

All irradiations were performed with 1.5 Mev electrons from a Van de Graaff accelerator. Typical beam currents in the 12 to 18 μampere range were employed for the 77K irradiations. For the helium irradiation a 10 μampere pulsed beam ('on' for 20 sec, 'off' for 40 sec) seemed to minimize sample heating.

Temperature Monitoring

Samples studied in the finger dewar required no monitoring since these samples were immersed directly in the liquid nitrogen. The stainless steel helium dewar was equipped with a gold-iron vs. chromel thermocouple attached to the bottom plate of the resonant cavity just below the sample. Because of a floating reference temperature, measured on top of the dewar, temperatures quoted in this dissertation must be viewed as approximate, perhaps ±2K tolerance.

During irradiation into the helium dewar, the temperature was constantly monitored with a microvolt digital voltmeter. The maximum sample temperature was conservatively estimated not to have been in excess of 35K.

Pulse Anneal Studies

Thermal anneal studies were achieved by two different methods. For the 77K irradiated samples, the Varian variable temperature system was used in conjunction with the V-4531 rectangular cavity. Tempera-

tures were monitored by a copper vs. constantan thermocouple. Samples were held at a fixed temperature for three minutes before returning to the base temperature (~86K) and recording the ESR trace.

The helium dewar anneal study was accomplished by constant monitoring of an ESR resonance line during warm-up after the helium had boiled off. In the 30 to 50 K range, the warm-up rate was ≈ 1 K/min; for the 50 to 70 K range, the rate was ≈ 1/2 K/min.

Ultraviolet Bleaching

Only those samples irradiated at 77 K were optically bleached. This was accomplished by bleaching into the finger dewar with a 100 watt high pressure mercury lamp. No attempt was made to bleach at a particular wavelength.

Spectrometer

The ESR spectra of the 77K irradiated samples were obtained with the same X-band homodyne spectrometer described by Rhoads (52). This instrument utilizes a 100 kHz modulation unit and a Schottky barrier detector diode. The magnet, maximum field ~4500 G, was a Varian six-inch current regulated model.

Spectra of samples irradiated in the helium dewar were taken with essentially the same microwave bridge but a larger magnet (Varian V-7200 with Mark I Fieldial). Microwave components for this system have been described by Little (53). For metal dewar studies, the modulation coils were external to the dewar tail (see Figure 4).

This latter change was made possible by a recently developed low noise back diode detector (Microwave Associate Model 41816). At low

modulation frequency (500 Hz) this back diode detector has much less inherent noise than the Schottky barrier diode.

Reduction in modulation frequency served to intensify another intrinsic problem with the helium dewar; that is, the microphonics problem. This problem was solved by changing to a stainless steel helium heat shield and three stainless steel stabilizing screws locking the nitrogen heat shield to the helium shield. (See Figure 4). While providing a small heat leak to the nitrogen heat shield, relative vibrational motion responsible for the microphonics was inhibited.

Static Field Measurement

Magnetic field positions were measured using the same NMR marginal oscillator as described by Rhoads (52).

CHAPTER V

EXPERIMENTAL RESULTS

Introduction

While this experiment has been very successful in terms of completion of its specific objective, namely, characterization of the V_K center in MgF_2, it has followed along paths considered unusual for the typical self-trapped hole experiments. Traditionally, following low temperature irradiation, spectra due to several defects are found. The task of separating and isolating the spectra of one particular defect requires much experimental finesse. Contrary to this normal behavior, one of the major obstacles incurred in the present work has been the production of an ESR spectrum. As has been previously implied, MgF_2 does not damage very easily.

This chapter will devote itself to presenting the experimental facts as they were determined. While analysis and discussion of data is the major topic of the next chapter, brief comments of minor points will be encountered frequently in this chapter.

Defect Production

The first sample irradiated during the course of this experiment was the small optical sample A1 (Table I). The sample was placed in the helium dewar, cooled to approximately 5K, and irradiated for 15

minutes (pulsed, 10 sec 'on' - 30 sec 'off'). No V_K type signals were observed as a result of this treatment. This failure was interpreted as a lack of electron traps. The sample was then irradiated for 7 hours (~15 μamperes) at room temperature; this treatment produced an easily measured ESR signal due to the F center. The sample was returned to the helium dewar for a second similar low temperature irradiation. However, this also failed to produce an observable V_K type spectrum. In an effort to increase sensitivity, only the larger samples listed in Table I were subsequently used. These samples represent, in most cases, the largest sizes acceptable by both the finger and metal dewar systems.

After prolonged irradiation (9½ hours) at 77K, an observable V_{KA} signal was obtained. Following this initial observation, the V_{KA} signal was produced in several crystals (A, C and E) having different mounting planes. The V_K spectrum was only slightly easier to produce; requiring at least 50 minutes pulsed-beam irradiation (beam current ≈10 μamperes) with the metal dewar. Sample temperatures were in the 5 to 35K range during the 50 minute irradiation.

V_K Experimental Spectra

The V_K center spectra obtained after the 5K irradiation will now be presented. Figure 5 taken with the magnetic field parallel to the c-axis, [001] direction, was obtained after 50 minutes of electron irradiation. Sample temperature, measured during irradiation was never in excess of 35K. ESR lines attributed to V_K centers occur around 2700 and 3600 G. The large center line and the two smaller lines (~ 3000 and ≈ 3500 G) are due to the grease used to mount the sample. The outer F center lines are observed around the large grease line. The V_K center

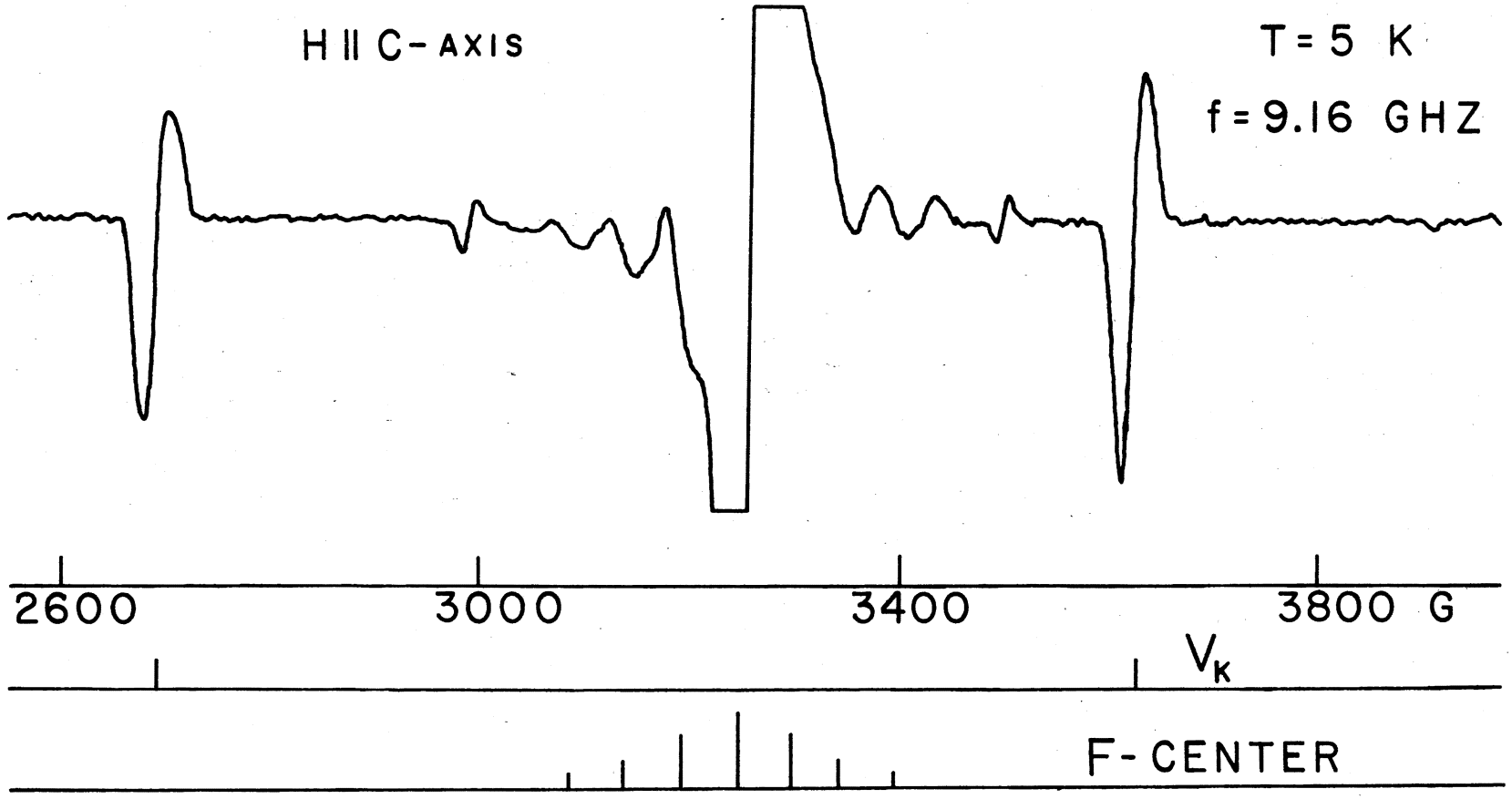

Figure 5. The [001] V_K Spectrum @ 5K; H || c-axis, Sample F

lines remain saturated at 5K even though the microwave power attenuator was turned down to 60 db. This saturation is illustrated in Figure 5 by the asymmetric line shapes for the V_K center.

The V_K center spectrum shown in Figure 6 was taken with the magnetic field parallel to the [110] direction. In this figure there are two V_K lines in the high field region as well as two V_K lines in the low field region. Because of a misalignment ($\approx 2^o$ or less) the V_K lines appear slightly split.

Table II summarizes the measured line positions for the V_K center when the magnetic field is along the [001] direction (c-axis) and the [110] direction (perpendicular to c-axis). Also included in the table are the calculated values based on the analysis of the next chapter.

V_{KA} Experimental Spectra

In this section, three experimental spectra will be presented. These spectra were taken along the three high symmetry directions ([001], [100], and [110]). Lines from the V_{KA} center, as well as from a S = 5/2 impurity, are observed in all spectra. The three samples utilized were electron irradiated simultaneously for 9½ hours (beam $\approx$ 20 μamperes) at liquid nitrogen temperature. All data reported in this section were obtained at 77K.

The V_{KA} center spectrum of Figure 7 was obtained with the magnetic field parallel to the c-axis ([001] direction). As expected for 77K observations, saturation effects of V_{KA} lines ($\approx$ 2700 and $\approx$ 3600 G) were not evident at 17 db microwave power level. A noticeable baseline drift was characteristic of the ESR spectrometer when operating at high microwave power and gain levels.

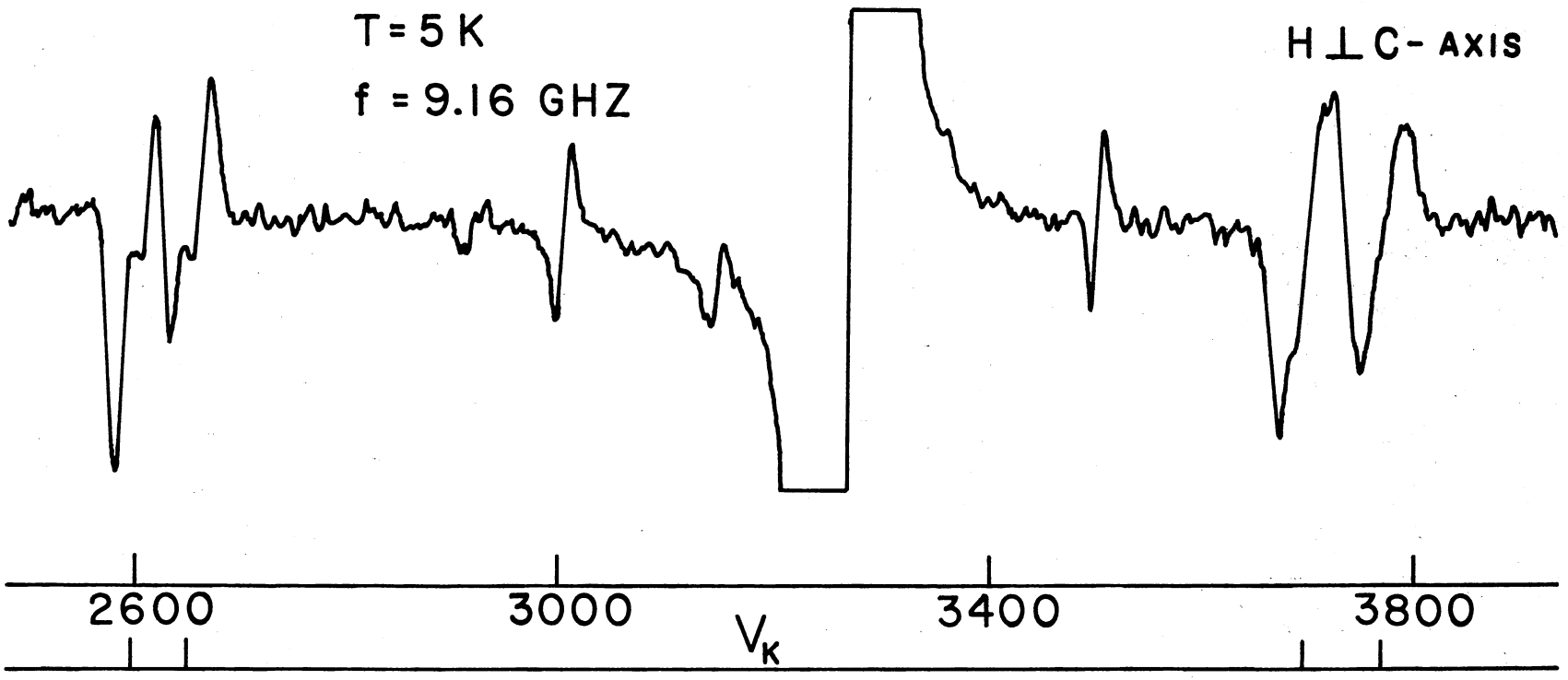

Figure 6. The [110] V_K Spectrum @ 5K; H $\perp$ c-axis, Sample F

TABLE II

CALCULATED AND MEASURED LINE POSITIONS (IN GAUSS)

Data	Sample	Measured	Calculated
(A). V_K Center; microwave frequency = 9.16457 GHz			
H $\|\|$ c-axis; [001]	F	2693.24	2691.62
		3626.55	3626.45
H $\perp$ c-axis; [110]	F	2592.59	2595.60
		2642.96	2643.12
		3696.19	3696.46
		3763.13	3763.17
(B). V_{KA} Center; microwave frequency = 9.17849 GHz			
H $\|\|$ c-axis; [001]	C	2703.12	2699.97
		3622.12	3619.04
H $\perp$ c-axis; [100]	A	2439.99	2442.05
		4030.76	4032.74
H $\perp$ c-axis; [110]	E	2584.51	2583.98
		2652.73	2655.33
		-------	3684.07
		3794.15	3792.26
(C). Impurity (Fe^{3+}) Spectra; microwave frequency 9.17849 GHz			
H $\|\|$ c-axis; [001]	A	1859.02	1858.85
		4700.78	4696.72
H $\perp$ c-axis; [100]	A (Site A)	2229.39	2226.66
		2537.06	2538.94
		2986.36	2990.28
		3619.82	3618.20
		-------	4659.00
H $\perp$ c-axis; [100]	A (Site B)	1944.70	1963.15
		2440.01	2449.69
		3041.36	3040.53
		3768.87	3776.59
		-------	4906.29
H $\perp$ c-axis; [110]	E	2089.32	2090.33
		2492.23	2495.08
		3020.35	3018.91
		-------	3698.92
		4772.52	4776.25

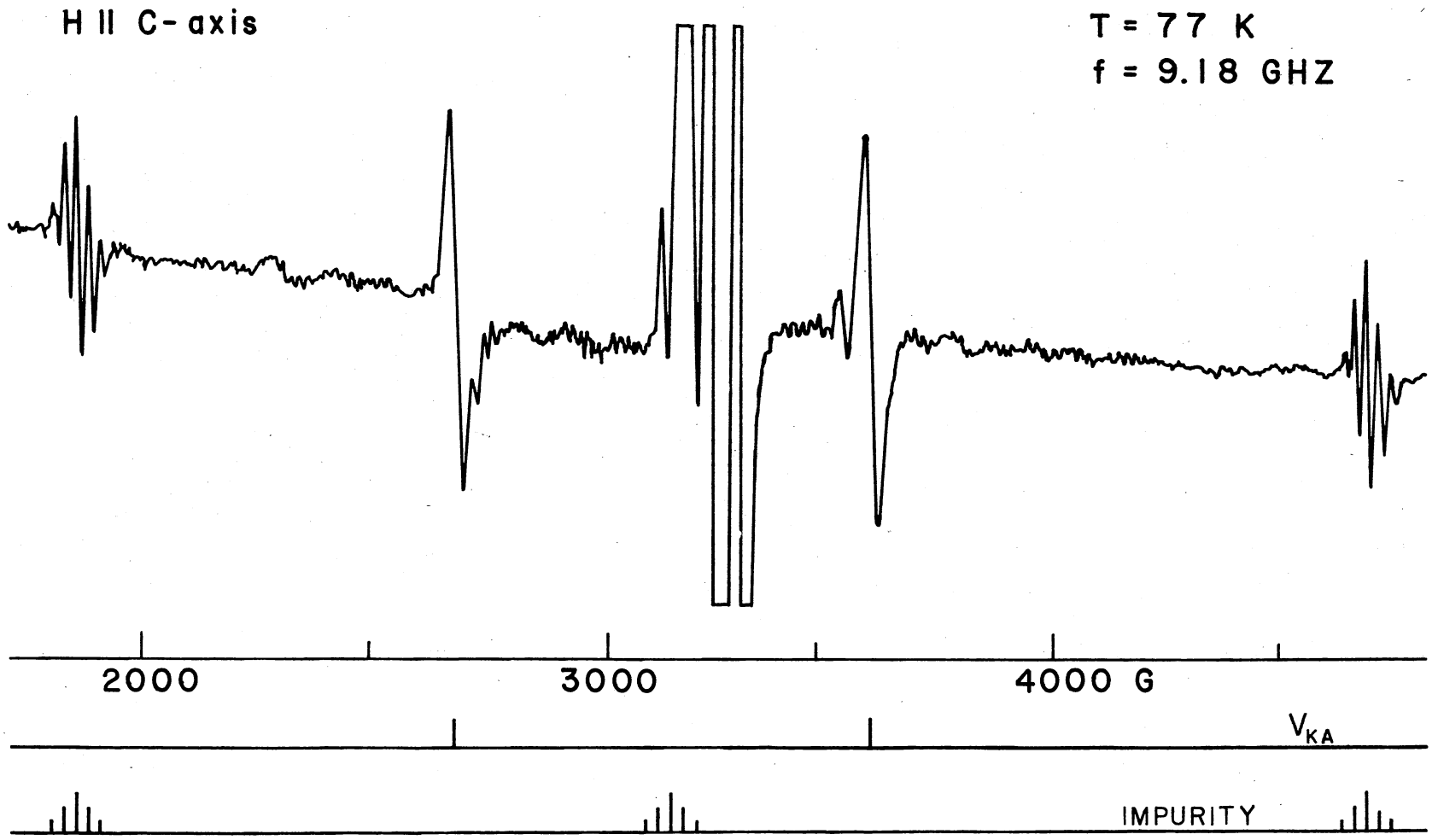

Figure 7. The [001] V_{KA} Spectrum @ 77K; H || c-axis, Sample C

Figure 7 also shows two (≈ 1850 and ≈ 4700 G) of the five groups of lines associated with the electronic spin 5/2 impurity ion; two of the groups fall outside the magnetic field range shown in this figure while the remaining group presumably lies under the large center line.

The central portion of this figure (centered around the free spin region) contains more than the inner V_{KA} lines and an impurity group. Operating the ESR spectrometer at reduced gain, the center line was found to be 3 lines with a 1:2:1 intensity ratio. Perhaps more surprising was the fact that the lines were isotropic. These large center lines were considered incidental to our present investigation; additional studies will be required before any identification is possible (although they are most likely impurity associated).

The spectrum of Figure 8 was obtained from sample E with the magnetic field parallel to the [110] direction. The two V_{KA} lines (≈ 2544 and ≈ 2653 G) on the low field side are well resolved while only one (~ 3794 G) is clearly observed on the high field side. The other high field line lies under the adjacent impurity group. All five impurity groups for this orientation are observable in Figure 8. One additional point is the identification of a barely resolved peak at 3138 G. This is most likely one of the inner V_{KA} lines.

In Figure 9 the magnetic field is parallel to the [100] direction (sample A). Note, this sample is believed to have a somewhat higher impurity concentration. Although the magnetic field is perpendicular to the c-axis, only two V_{KA} lines (≈ 2440 and ≈ 4031 G) are clearly resolved. For this particular orientation, the impurity groups can be separated into two classes. All five groups of one class are observable (~ 2229, ≈ 2537, ≈ 2986, ≈ 3619 and ≈ 4700 G) while 4 of the groups from the

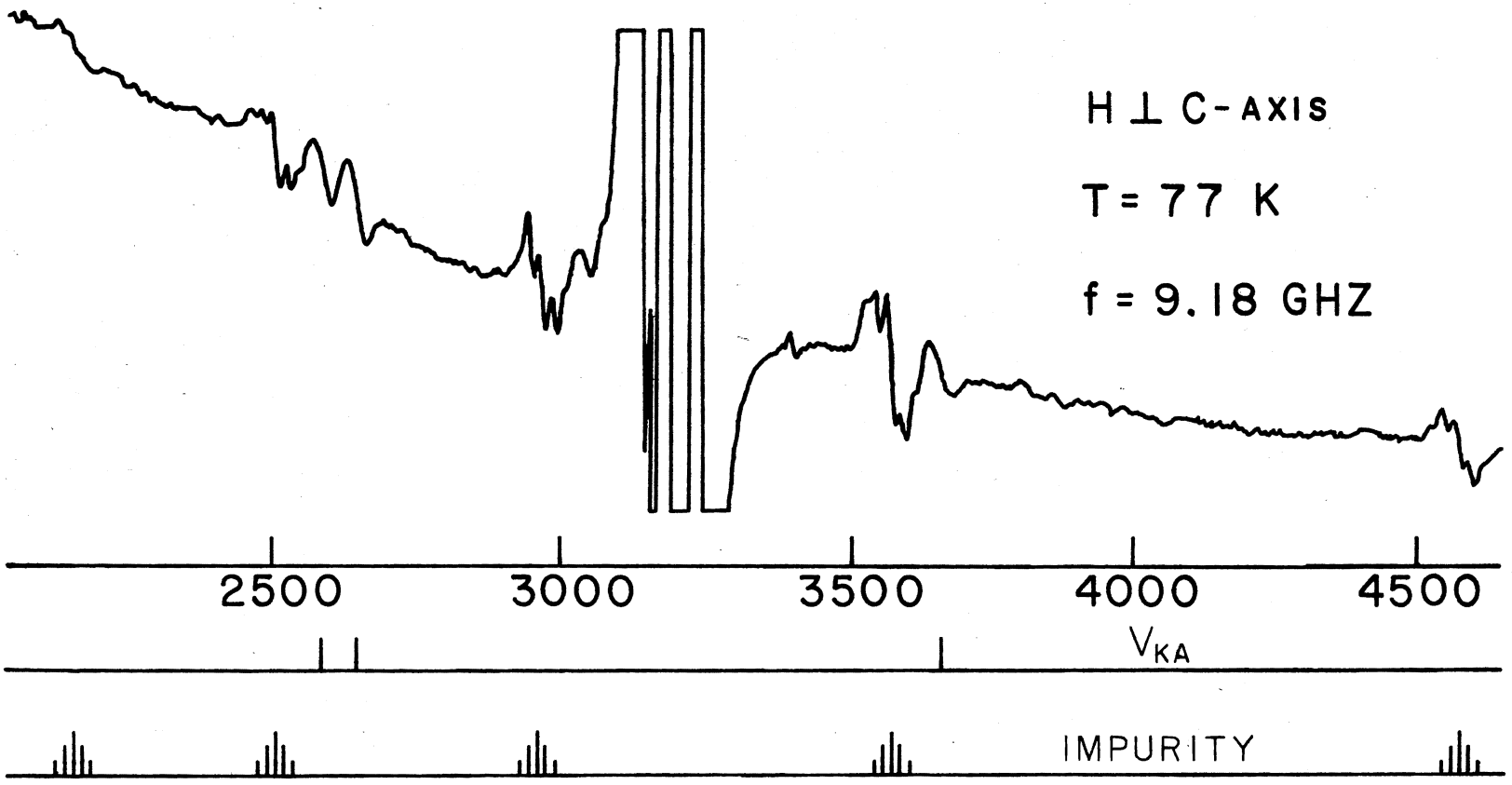

Figure 8. The [110] V_{KA} Spectrum @ 77K; H $\perp$ c-axis, Sample E

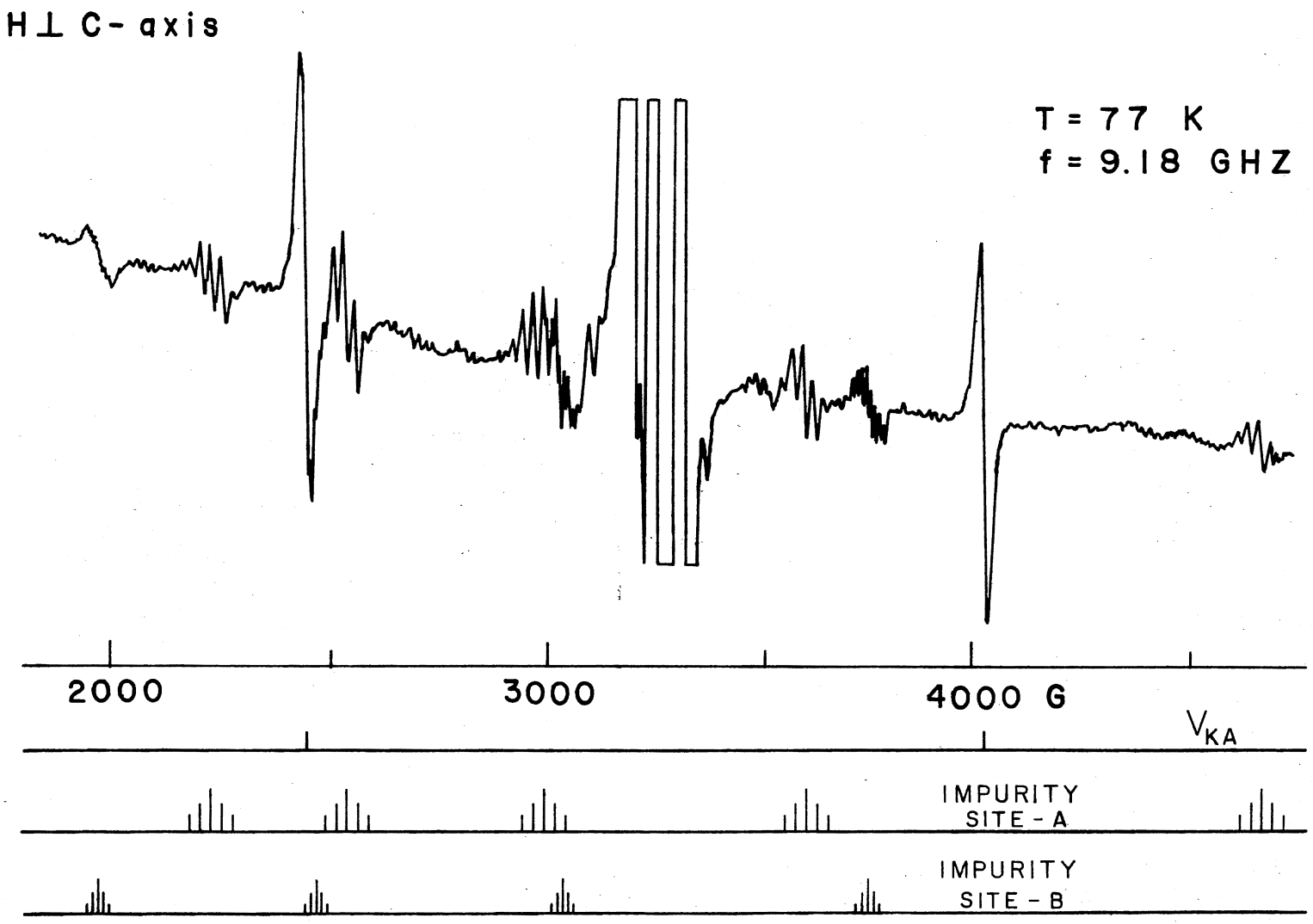

Figure 9. The [100] V_{KA} Spectrum @ 77K; H⊥c-axis, Sample A

other class are observable (≈ 1945, ≈ 2460, ≈ 3041 and ≈ 3769 G).

Table II also contains V_{KA} line positions along the previously mentioned high symmetry directions and the calculated values as determined in the next chapter for comparison.

Thermal Anneal Studies

One of the most important parameters associated with color centers is the so-called decay temperature. This can be more precisely expressed in terms of an 'activation energy' for a given process. Physically, the decay temperature represents that temperature at which the defect becomes mobile.

In order to determine this temperature for the V_{KA} center, a sample previously irradiated at 77K and maintained at this temperature was quickly transferred into the Varian variable temperature accessory previously described. Figure 10 shows the results of the subsequent pulse-anneal experiment. The sample was maintained at the elevated temperatures, represented by the points, for three minutes before cooling back to the base temperature (in this case ≈ 86K) for measurement. The peak-to-peak amplitude of the low field line in Figure 7 has been plotted in Figure 10 as a function of temperature. A significant observation during the V_{KA} anneal study was a pronounced broadening of the V_{KA} lines as a function of temperature. In going from 86 to 93K, the amplitude of the lines were reduced by approximately a factor of three.

The data represented by Figure 11 were obtained by continuously monitoring the sample temperature while repeatedly measuring the peak-to-peak amplitude of the high field line in Figure 5. The dotted curve

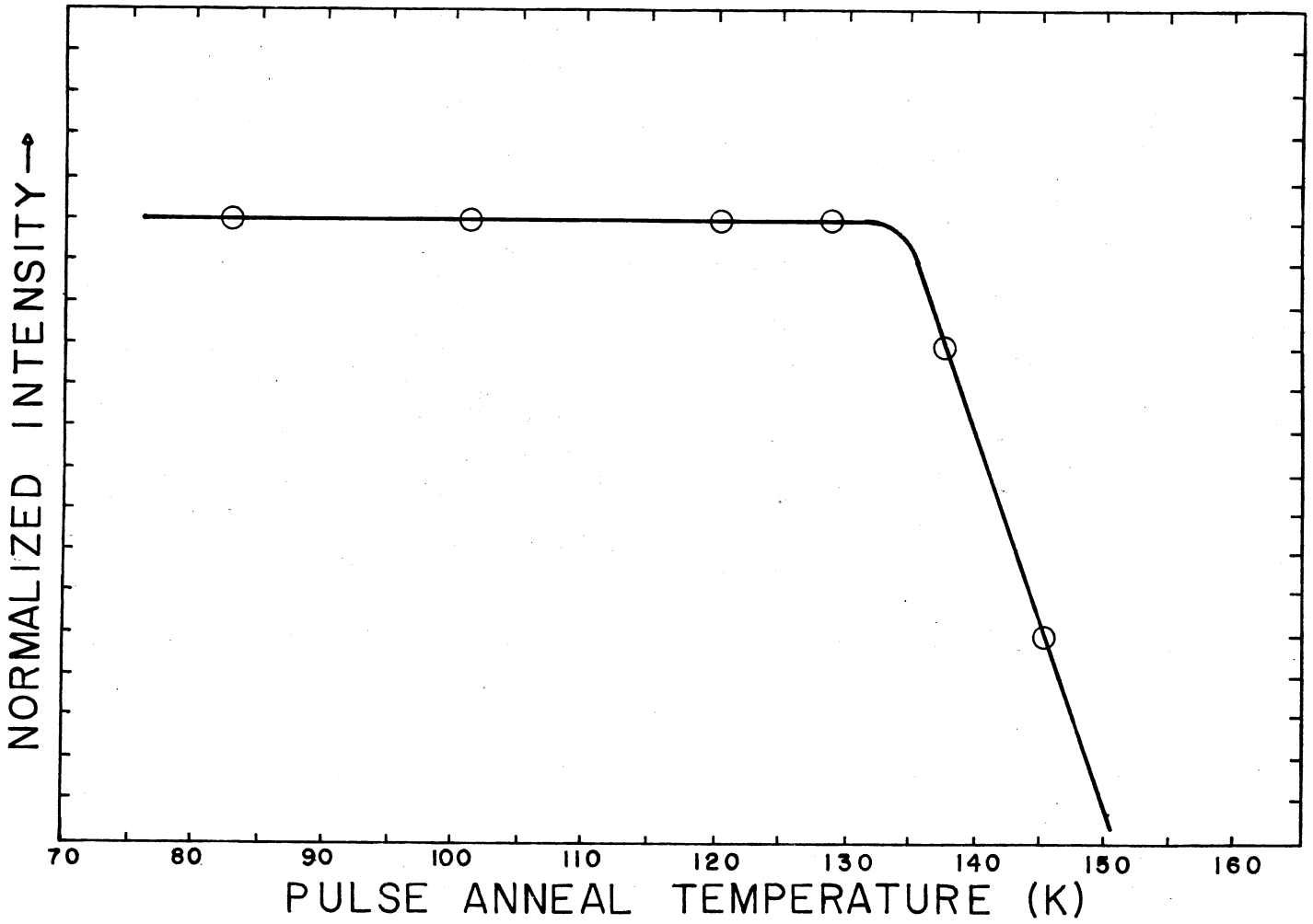

Figure 10. Pulse Anneal Decay of the V_{KA} Center in MgF_2

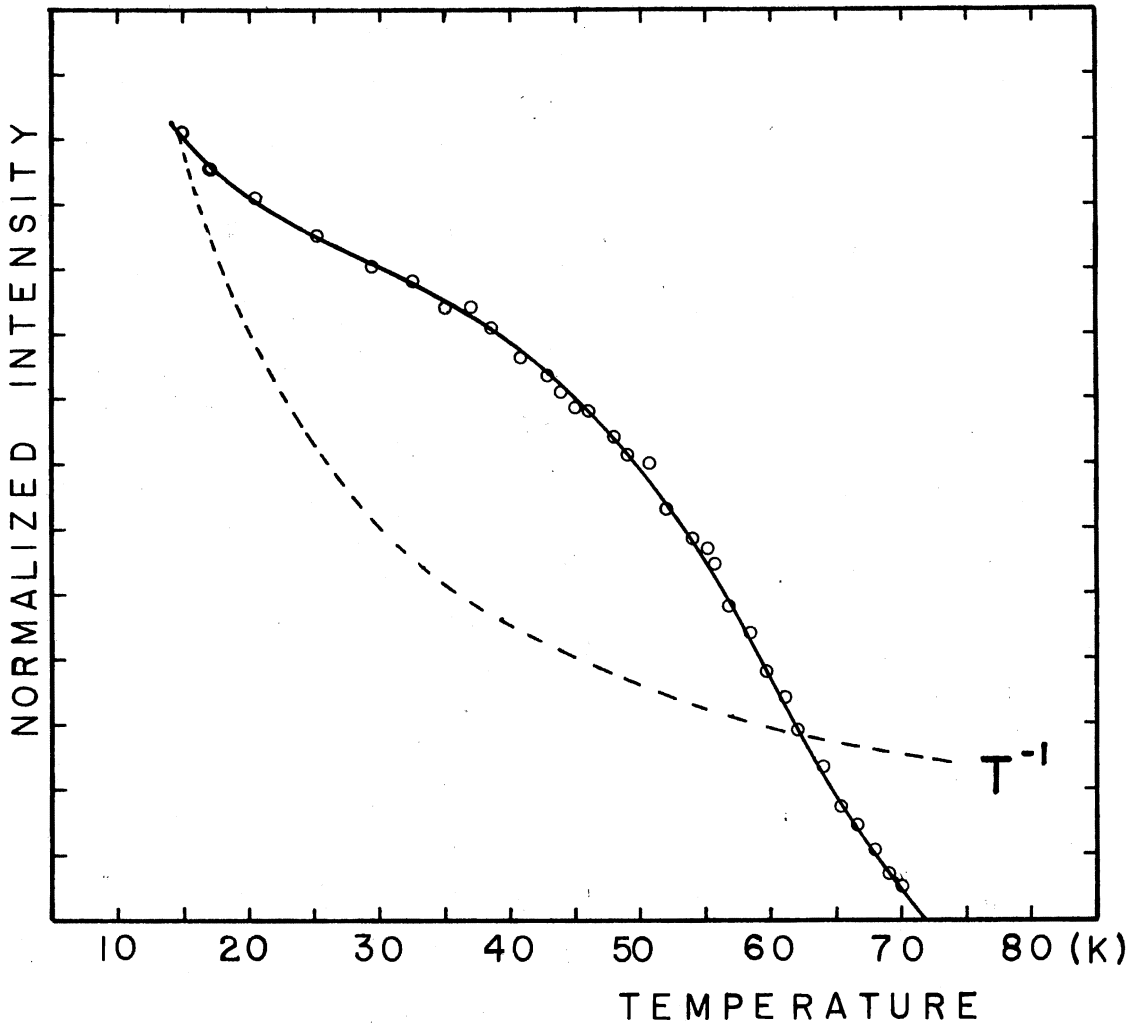

Figure 11. Continuous Thermal Decay of the V_K Center in MgF_2

is a reciprocal temperature plot which has been normalized to the lowest temperature point. This represents the normal decrease in signal due to the Boltzmann factor.

Ultraviolet Bleaching

Experiments described in this section were restricted to finger dewar samples C and A. After all line positions were measured, sample C was bleached for 4 minutes at 77 K as described in Chapter IV. The monitored high field V_{KA} line of Figure 7 was not affected by this bleach. However, the S = 5/2 impurity lines disappeared. Similar results were obtained for the V_{KA} lines recorded from sample A; both 'classes' of impurity groups in Figure 9 were observed to decay as a result of this bleaching procedure. The sample was warmed to room temperature (orange thermoluminescence observed). A 5 minute irradiation at 77 K regenerated some of the V_{KA} spectra and most of the impurity associated spectrum.

CHAPTER VI

ANALYSIS AND DISCUSSION

Introduction

The V_K center is normally the first defect to be produced in a halide material by low temperature irradiation. Since only one fluorine molecular-ion spectrum was observed in Figures 5 and 6, it has been attributed to the V_K center. The decay temperature and angular data as discussed in this section provide verification of this assignment. Final characterization of the V_K center consists of determining its spin Hamiltonian parameters.

Analysis of V_K Spectra

A V_K center is formed whenever two neighboring fluorine ions share a hole. In the case of MgF_2 there are four nearest neighbor fluorine combinations as shown in Figure 1. These have C_{2h}, C_{2v}, D_{2h} and C_1 symmetries respectively. Which of these sites is populated can be determined from the angular dependence of the V_K center ESR spectrum. As with all fluorine molecular-ions, the crucial parameter determining the angular dependence is the angle between the molecular-ion axis and the applied magnetic field. For example, the hyperfine lines created by the fluorine nuclei have their maximum splitting (approximately 1800 G) when the magnetic field is parallel to the molecular axis and their

minimum splitting (approximately 150 G) when the field is perpendicular to the molecular axis. Referring to Figure 5, one sees only one pair of V_K center lines which indicates that all the V_K centers are equivalent for this orientation of field parallel to the c-axis. In addition, the splitting of this pair is approximately 934 G which indicates the angle between the magnetic field and the fluorine molecular axis is within the 40-50^{o} range. Of the four possible V_K center sites, only the site having C_1 symmetry can account for the observed spectrum. The other three sites either make an angle of 0^{o} or 90^{o} with the magnetic field for this [001] orientation and thus are clearly eliminated as possible sites.

The spectrum shown in Figure 6, with the magnetic field parallel to the [110] direction, further confirms the conclusion reached in the preceeding paragraph concerning the populated site. For this orientation of the magnetic field, the C_1 symmetry sites are not equivalent between the two octahedra at right angles to each other (see Figure 2). The molecular axis of the V_K center located in the C_1 symmetry site on one octrahedon makes a slightly different angle with the magnetic field than does the corresponding molecular axis on the other octrahedron. Although different, these angles are still in the 40-50^{o} range. Therefore one expects two pairs of V_K center lines with slightly different splittings for spectra taken with this [110] direction of magnetic field. These two pairs are observed in Figure 6.

Another argument in support of the C_1 symmetry V_K center site is based on inter-nuclear separations. If the fluorine-fluorine distance is too large, the V_K center will never be formed initially. If the separation is too small, there will be insufficient lattice distortion

upon formation, thus causing the V_K center to have a very low decay temperature. The C_{2h} symmetry site has a larger separation and the D_{2h} symmetry site has a smaller separation than the C_1 site. Hence, these would most likely be unstable for the reasons just cited. The F-F distance for the C_1 symmetry site in the perfect MgF_2 lattice is nearly identical to the F-F separation in LiF and $KMgF_3$.

From Figure 11, after taking into account the drop in intensity due to the Boltzmann factor, one finds a decay temperature for the V_K center in the 55-65 K range. This temperature is somewhat lower than the analogous decay temperature for V_K centers in LiF and $KMgF_3$. In both of these latter materials, the V_K center decays at approximately 110-120 K (54,55). The lower decay temperature for MgF_2 is a result of a lower activation energy for jumping. From inspection of the lattice, it is apparent that jumps from one C_1 symmetry site to another along the c-axis are unhindered and should have a low activation energy. This is only the second material known to have the intrinsic V_K center mobile below 77K, the first being NaI (55).

The following spin Hamiltonian was used to describe the V_K center spectra (56).

$$H = \beta \vec{H} \cdot \overleftrightarrow{g} \cdot \vec{S} + \vec{I}_1 \cdot \overleftrightarrow{A}_1 \cdot \vec{S} + \vec{I}_2 \cdot \overleftrightarrow{A}_2 \cdot \vec{S} - g_N \beta_N \vec{H} \cdot (\vec{I}_1 + \vec{I}_2) \quad (2)$$

where $\vec{S}$ and $\vec{I}$ are the electron and nuclear spin operators respectively; β and β_N are the Bohr and nuclear magnetron respectively; $\overleftrightarrow{A}_i$ represents the hyperfine tensors for the two fluorine nuclei. In Equation (2), the first term is the electronic Zeeman, the next two terms represent the hyperfine interactions, and the last term is the nuclear Zeeman.

The principal values of the $\overleftrightarrow{g}$ and $\overleftrightarrow{A}$ tensors, as well as the directions of the principal axes are the parameters to be determined. One of the principal axes for each tensor has been assumed perpendicular to the plane formed by the two fluorines comprising the V_K center and the nearest neighbor magnesium (see Figure 12). In analogy with $KMgF_3$ (57), a bent-bond angle, $\varepsilon = 7^{\circ}$, was used in all calculations although there was no experimental evidence to substantiate this assumption. Also, the hole was assumed to be equally shared between the two fluorines, and this effectively removed any importance connected with the occurrence of a bent-bond.

Because of the low symmetry of the rutile structure, the lattice distortion associated with the formation of the V_K center will cause the molecular ion axis to deviate slightly from the direction of the initial F-F axis before V_K formation. Thus the two angles, α and β (illustrated in Figure 12) characterizing the orientation of the molecular axis relative to the lattice will be determined from the experimental data.

Since only six experimental line positions were measured (see Table II) for the V_K center, the parameters g_z, A_z, α and β will be determined from the data, and appropriate values will be assumed for the other parameters during all calculations. Assuming values for these latter parameters is not a serious limitation as they seldom vary by more than a few percent from one material to another. In fact, angles α and β represent the only significant new information in so far as MgF_2 is concerned.

The spin Hamiltonian, given in Equation (2), was put in a form more amenable to analysis by the following procedure. First, the spin Hamiltonian was expressed in terms of the principal axis coordinate

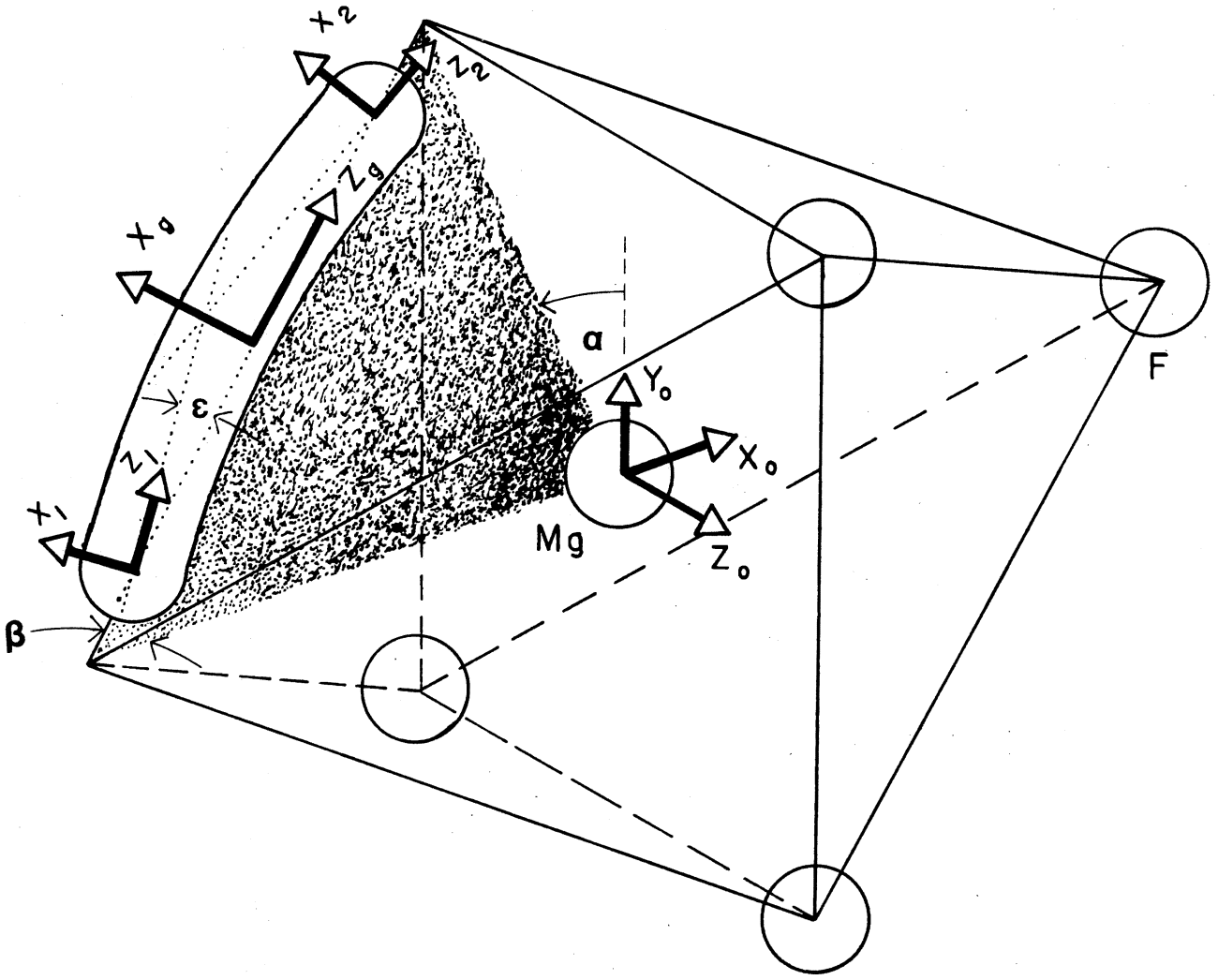

Figure 12. Model of V_K Center: Principal Axis System Noted

system of each of the individual tensors (see Figure 12). Then the separate coordinate systems were transformed into a common magnetic field coordinate system, defined as having the field along the z-axis. Finally, the Hamiltonian was written as an eight by eight complex Hermitian matrix using the $|M_S, M_{I_1}, M_{I_2}>$ spin manifold. The eigenvalues were obtained from this matrix by computer diagonalization techniques (see Appendix G, Rhoads (52)).

Two distinct yet essentially similar computer programs were used. In one, the values for the spin parameters were provided to the computer, and the program determined the line positions as a function of magnetic field direction. This was accomplished by an iteration process in which the magnetic field was varied until the energy separation corresponded to the microwave frequency. Examples of this type program will now be considered in greater detail.

Figure 13 represents a computer generated angular behavior of the V_K center for sample C. In this case, the mounting plane was a $(\bar{1}10)$ plane and the magnetic field could be rotated from c-parallel [001], to c-perpendicular [110]. Note how the inner and outer lines split as one rotates off the high symmetry [001] direction. For c-perpendicular ($\phi = 0^o$) the calculated splittings at low and high fields were 73 and 102 G; experimentally observed splitting were 70 and 105 G respectively. Figure 14 shows the angular behavior for rotation of the magnetic field in the basal or (001) plane. For reasons previously mentioned only the outer V_K center ESR lines were measured in this investigation. Similar comments equally apply to Figure 15. This latter angular behavior was experimentally confirmed in the spectra of sample A.

In the second program, the line positions were given to the computer

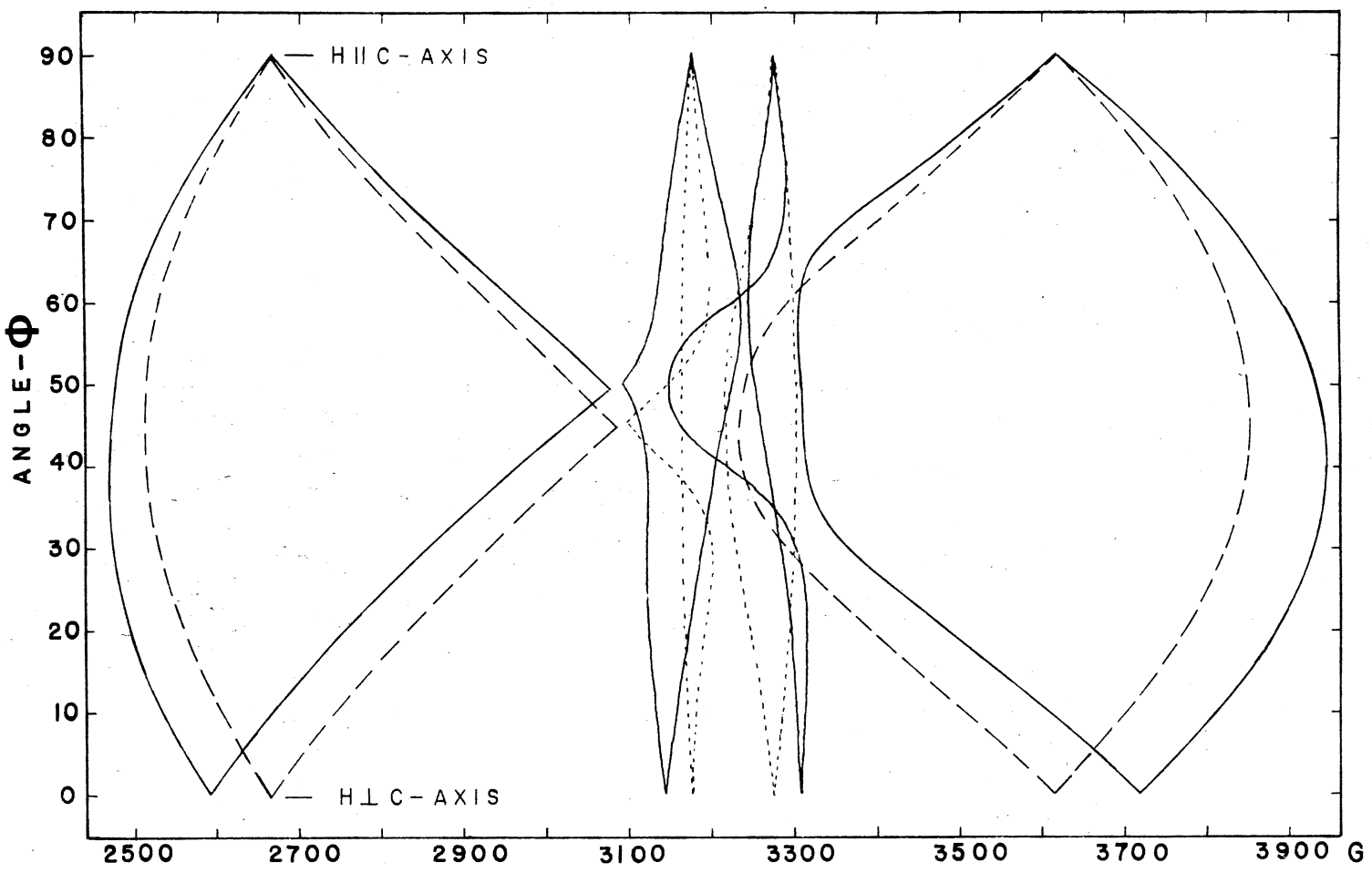

Figure 13. Computer Generated Angular Study of Self-Trapped Hole Center in MgF_2: Rotation in $(\bar{1}10)$ Plane

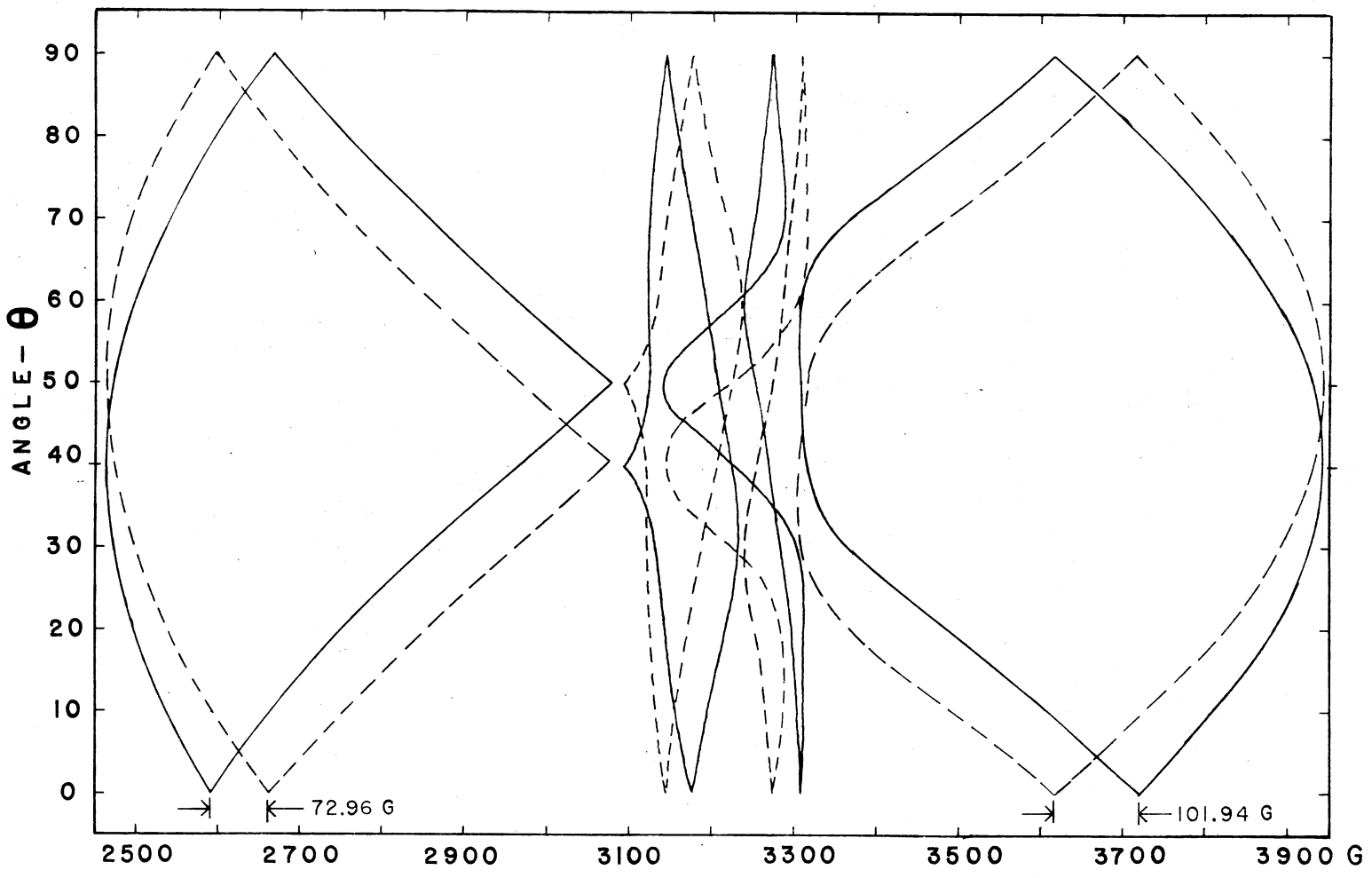

Figure 14. Computer Generated Angular Study of Self-Trapped Hole Center in MgF_2: Rotation in (001) Plane

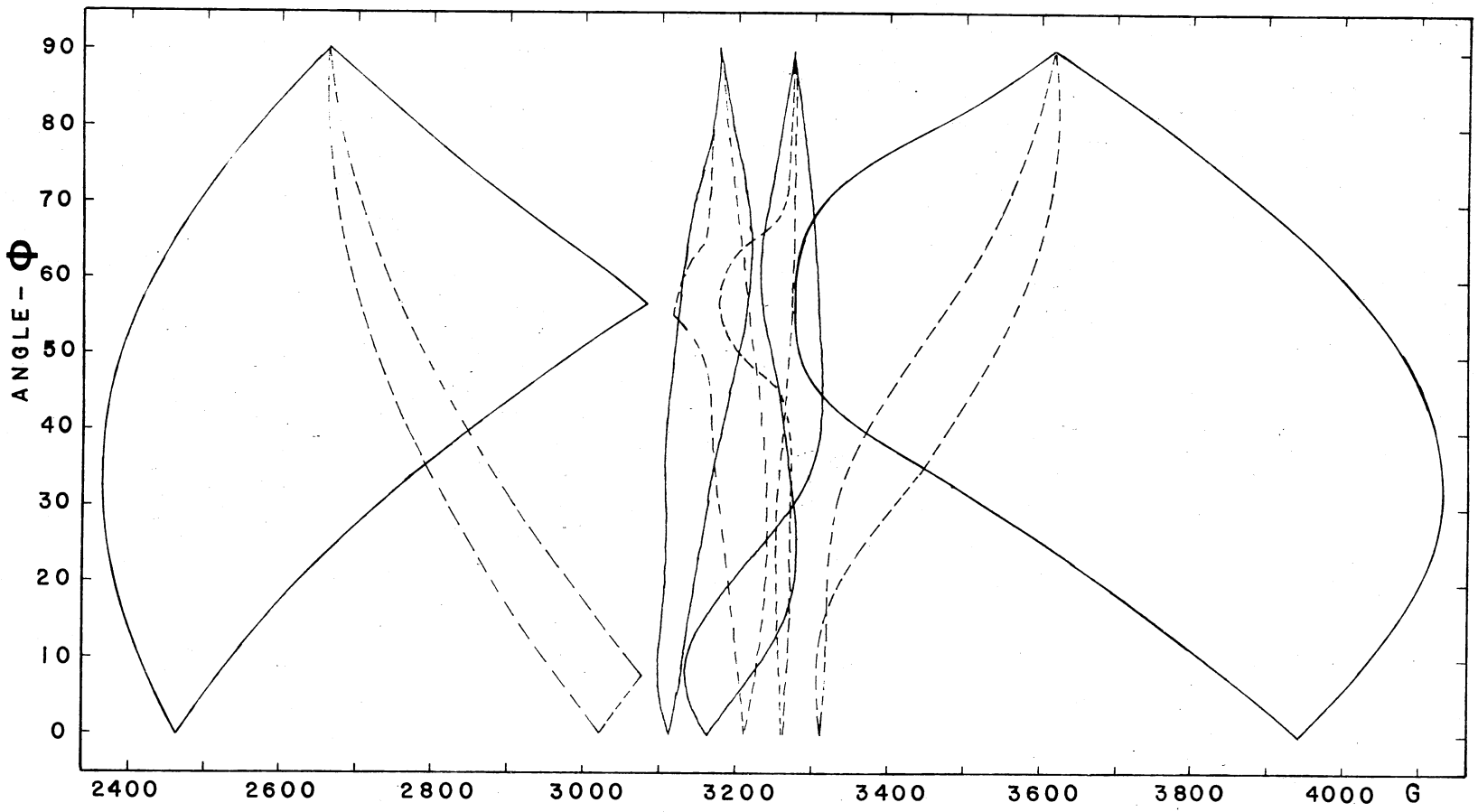

Figure 15. Computer Angular Study of Self-Trapped Hole Center in MgF_2: Rotation in (010) Plane

and the program determined the best set of spin parameters. Initial values of the parameters were used to calculate a quantity called SUM which was a sum of the squares of the deviations of the experimental microwave frequency from the computed microwave frequency corresponding to each line. The parameters were systematically varied by the computer to minimize SUM. The values determined by this procedure, g_z, A_z, α and β are listed in Table III.

The values obtained for g_z and A_z correspond to the normally expected values (55). Values obtained for α and β should be compared to those of the perfect lattice, $\alpha = 39.9^o$ and $\beta = 41.1^o$ respectively. Thus one observes an easily measurable lattice distortion associated with the V_K center because of the low symmetry of the MgF_2 lattice.

Analysis of V_{KA} Spectra

The name 'V_{KA} center' is used to designate an impurity associated V_K center. Normally, these V_{KA} centers are created in one of two ways; (a) V_K centers may be produced then the sample temperature is raised above the temperature of mobility at which time the V_K migrates to the impurity or (b) the sample may be irradiated at a temperature for which the V_K is already mobile. The V_{KA} centers reported in this dissertation were produced by the latter method. Normally, spectra due to the V_K and V_{KA} centers are nearly indistinguishable since, to first order, all fluorine molecular-ion systems are independent of the host lattice (58). The most prominent difference between the intrinsic and perturbed hole centers is their thermal stability; this being the usual way of distinguishing between the two centers.

The V_{KA} center occupies the same C_1 symmetry site as its parent V_K

TABLE III

SPIN HAMILTONIAN PARAMETERS

(A).	V_K Center
	$g_x \cong g_y = 2.020 \pm 0.0005$
	$g_z = 2.0022 \pm 0.0005$
	$A_x \cong A_y = 100 \pm 50$ MHz
	$A_z = 2602 \pm 10$ MHz
	$\alpha = 48.4^{\circ} \pm 0.3^{\circ}$
	$\beta = 39.7^{\circ} \pm 0.3^{\circ}$
(B).	V_{KA} Center
	$g_x \cong g_y = 2.020 \pm 0.0005$
	$g_z = 2.0033 \pm 0.0005$
	$A_x \cong A_y = 100 \pm 50$ MHz
	$A_z = 2611 \pm 10$ MHz
	$\alpha = 48.4^{\circ} \pm 0.3^{\circ}$
	$\beta = 41.1^{\circ} \pm 0.3^{\circ}$
(C).	Impurity (Fe^{3+}) Spectra
	$g = 2.0019$
	$\lvert D \rvert = 1991$ MHz
	$\lvert E \rvert = 62$ MHz

center. This conclusion follows by applying the same arguments used for Figures 5 and 6. With the magnetic field parallel to the [001] direction (c-axis) as in Figure 7, all of the V_{KA} centers are equivalent and give rise to a single pair of lines. For the magnetic field along the [110] direction, the V_{KA} centers on the two octrahedra at right angle to each other are inequivalent and thus give rise to two pairs of lines having slightly different splittings as shown in Figure 8. In the case of the magnetic field along the [100] direction, the V_{KA} center on a given octrahedron can be separated into two classes according to the angle between the molecular-ion axis and the magnetic field. These two angles are approximately 30 and 90^{o}; this gives rise to a widely split pair of lines and another only slightly split pair of lines. The widely split pair is readily observable in Figure 9 while the slightly split pair is obscured by the large center impurity lines.

Although spectra have been shown only for high symmetry directions, additional data have been obtained at various angles in the planes of rotation listed in Table I. The lifting of orientational degeneracy upon rotating off high symmetry directions provided further verification of our assignment for the V_{KA} center site. Figures 13, 14, and 15 also represent the approximate angular variation of the V_{KA} center for rotation in high symmetry planes.

The V_{KA} center decays at ≈ 140 K (see Figure 10). This value, obtained by monitoring the low field V_{KA} line of Figure 7, is approximately the same as that reported (59) for the V_{KA} center in NaF (≈ 150 K). While monitoring the decay of the V_{KA} center a significant line broadening over a small temperature interval (≈ 7 K) was observed. In view of the reorientation effects reported (60) in $KMgF_3$, this broadening was

attributed to a reorientation (without migration) of the self-trapped hole about the impurity site.

Verification that the spectra of Figures 7, 8 and 9 have been correctly identified as arising from a V_{KA} center rather than the intrinsic hole center was obtained by an ultraviolet bleach experiment. The defect reported in these figures did not decay following an ultraviolet bleach at 77K.

In addition to substantiating the V_{KA} center assignment, ultraviolet bleaching provided information concerning the nature of the perturbation involved. A 4 minute bleach at 77K destroyed the impurity spectrum of Figure 9 but did not affect the V_{KA} spectrum. Even after a 30 minute bleach, the V_{KA} spectrum was still unaffected. Since the impurity spectrum is most likely due to Fe^{3+} (verification to follow), the bleaching is believed to release electrons, thus converting the Fe^{3+} into Fe^{2+}. Based on this assumption, the failure of the V_{KA} center to trap these released electrons indicates the effective charge of the V_{KA} center is either neutral or negative. The V_{KA} center would have this effective charge if the perturbation were a monovalent impurity ion or vacancy respectively. The effective charge of the intrinsic V_K center is positive.

This assignment of a monovalent cation or vacancy as the stabilizing perturbation for the V_{KA} center agrees quite well with the previously discussed motional effects. With this model (see Figure 16) there would be an electrostatic binding between the trapped hole and the perturbation. This would permit the very rapid reorientation about the perturbation while preventing migration of the hole away from the perturbation.

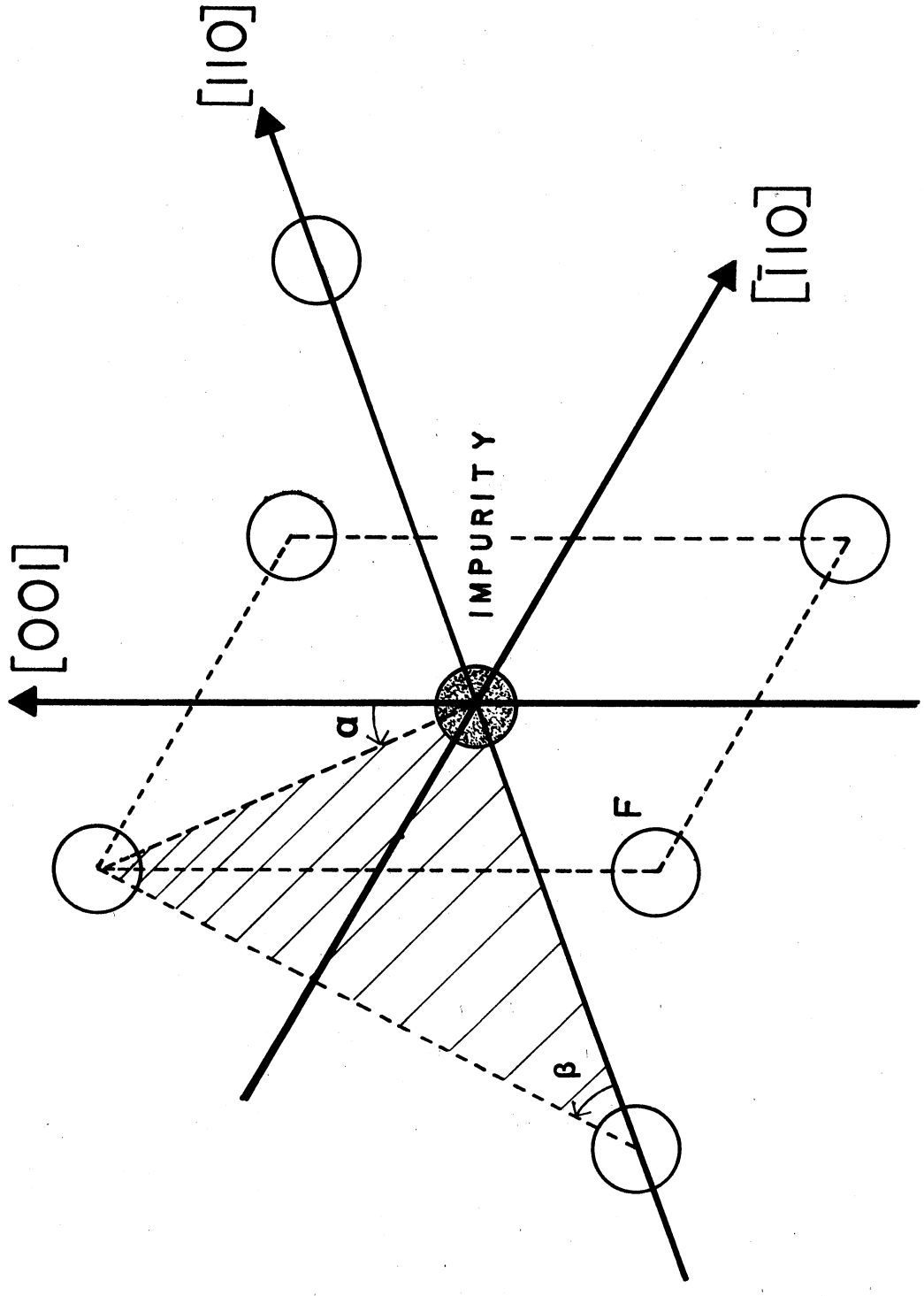

Figure 16. Model of V_{KA} Center

A spin Hamiltonian identical in form to Equation (2) was used for analysis of the V_{KA} center spectra. Spin Hamiltonian parameters were determined in the manner previously described and are listed in Table III. The V_{KA} parameters are very similar to the V_K parameters as expected. Spin Hamiltonian parameters for the V_{KA} center were based on more data (Table II) than were the corresponding parameters for the V_K center.

Analysis of Impurity Spectra

In the previous chapter the experimentally obtained V_K and V_{KA} spectra were presented in addition to two different types of impurity spectra. These two types were referred to as (A) 'groups of five lines associated with a spin 5/2 impurity' and (B) 'three line spectrum centered around $g \approx 2$ with intensity ratio 1:2:1'. In the following paragraphs, a brief analysis of the type A impurity spectrum (hereafter referred to as simply the impurity spectrum) will be presented.

Consider the impurity spectrum of Figure 7. Again, all five 'groups' (intensity ratio 5:8:9:8:5) of lines are not present for the reasons previously cited in Chapter V. There is no obvious hyperfine structure associated with this impurity spectrum. This implies that the impurity has an extremely small or zero nuclear magnetic moment. One other obvious observation is that within each group there are 'superhyperfine lines'. This structure results from the interaction of the electronic spin of the paramagnetic impurity with the nuclear magnetic moment of the surrounding six fluorine nuclei. No attempt will be made to analyze this superhyperfine structure.

Production efficiency of the impurity spectrum is extremely low.

As previously noted, this is a general statement (for low temperature irradiations of MgF_2) applicable to all observed defects rather than being specific to only the impurity spectrum. Confirmation of this generalization requires no more than an inspection of the spectra of Figures 7, 8 and 9 (9½ hours irradiation @ ≈ 20 μamperes) and the spectra of Figures 5 and 6 (50 minutes irradiation @ ≈ 10 μamperes). The impurity spectrum is not even present in the 50 minute irradiated samples.

The exact identification of the impurity itself lies outside the scope of this investigation (specific objective being the study of the self-trapped hole in MgF_2). However, other investigations [MgF_2:Eu^{3+} (61); MgF_2: Cr^{3+} (62); MgF_2:Mn^{2+} (63); MgF_2:V^{2+} (64)], leave little doubt that our impurity is one of the transition metal ions substituting for Mg^{2+}. Because of the 5/2 electronic spin, possible candidates are Fe^{3+}, Mn^{2+} and Cr^{1+}. The most likely candidate is Fe^{2+} substituting for Mg^{2+} which, upon irradiation, is converted to the observed S = 5/2 system, namely, Fe^{3+}. However, Cr^{1+} cannot be completely ruled out. The absence of any hyperfine structure in our spectra would eliminate the Mn^{2+} candidate since it has a 100% abundant magnetic isotope.

With the magnetic field parallel to the [001] direction, Figure 7, there exists only one 'class' of superhyperfine lines. That is, with the magnetic field parallel to the [001] direction, sites A and B (Figure 2) are magnetically equivalent. A 90° rotation of magnetic field, spectrum of Figure 9, produced the two different 'classes' of superhyperfine lines. Magnetic sites A and B are inequivalent for this latter orientation of magnetic field.

Additional information concerning the origin of the impurity

spectrum is obtained from the principal axis system for the zero-field interaction represented by E and D. Turning points in the spectrum will occur whenever the magnetic field is along any one of the principal axes. In Figure 7 the splitting between groups is a maximum. Therefore, the [001] direction is <u>one</u> of the principal axes.

Crystal symmetry would suggest the [110] and [$\bar{1}$10] as the other two principal axes. However, the computer was unable to find a 'fit' for the spin Hamiltonian (65)

$$H = g \beta \vec{H} \cdot \vec{S} + \vec{D}[S_z^2 - 1/3\ S(S+1)] + E\ (S_x^2 - S_y^2) \qquad (3)$$

and the measured line positions of Table II with this particular choice of principal axes. Agreement between 'calculated' and 'measured' line positions was obtained using the principal axes of Figure 17. Spin parameters determined with this principal axes system [100], [010] and [001] are reported in Table III. This particular choice suggest the presence of a perturbation in the [100] direction.

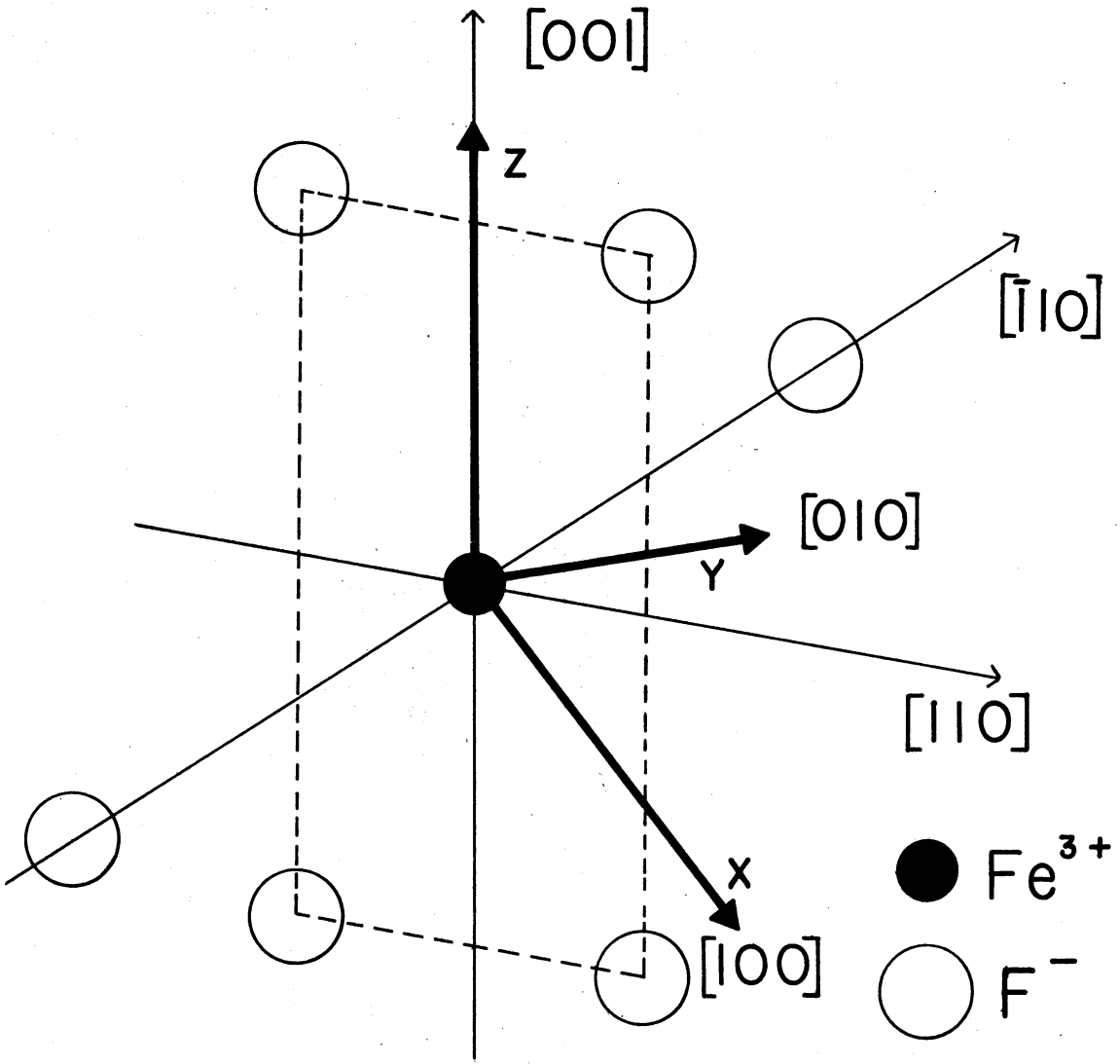

Figure 17. Model of Impurity Associated Center: Principal Axes Noted

CHAPTER VII

SUMMARY

Isolated point defects have been induced in single crystals of MgF_2, a rutile structured material. These defects, produced by 1.5 Mev electron irradiation at 5K and 77K, were investigated by ESR techniques.

Five different ESR spectra were observed during the course of this study. They were the F center, V_K center, V_{KA} center, a spin 5/2 impurity, and an unidentified impurity. Of these, only the F center ESR spectrum had been previously reported. The V_K, V_{KA} and spin 5/2 impurity spectra were analyzed.

Utilizing only the outer ESR resonance lines, detailed models of the self-trapped hole centers, V_K (Figure 12) and V_{KA} (Figure 16), have been obtained. Experimental conditions and the position of the yet unidentified impurity lines (centered about g ~ 2) prevented measurements of the inner V_K lines. This limitation, while not affecting the proposed models, prevented measurement of the 'bent bond' angle ε Figure 12. Exact line positions for the outermost lines were measured for three different directions of the magnetic field. Using computer diagonalization techniques, these line positions were converted into the spin Hamiltonian parameters given in Table III.

Similar line position measurements and calculations of spin parameters associated with the 5/2 spin impurity are summarized in Tables II and III respectively. While positive identification of the impurity

itself awaits a complete ENDOR analysis, supporting arguments for Fe^{3+} as the impurity have been presented.

Thermal anneal studies have yielded values of ~60K and ~140K for the decay temperature of the V_K and V_{KA} centers respectively. While 60K is a bit low, compared to alkali halide crystals, it is not believed too low for this particular structure (very open, low symmetry).

Extremely large irradiation doses were required to produce measureable concentrations of defects at the 77K irradiation temperature. Two possible explanations for this low damage efficiency are: (A) lack of electron traps and (B) the "openness" of the lattice itself. That is, the lattice is amenable for 'defect jumping' along the c-axis. Stated differently, while the damage process is the highly efficient Pooley-Hersh mechanism (15,16,17), back reactions <u>during</u> irradiation itself could severely limit the number of stable defects observed <u>after</u> irradiation. Unfortunately, back reactions are a transient phenomenon not easily accessible to direct measurement.

Suggestions for Further Work

Prior to this study the only defects reported in MgF_2 were the F and M centers. Since the ground state of the M center is not paramagnetic, only the F center has an ESR spectrum. Kolopus et al. have successfully correlated the optical and ESR spectra associated with the F center (50). A similar study, that is, correlation of the optical and ESR spectra associated with the V_K and V_{KA} centers would further elucidate the work reported in this dissertation.

Defect mobility has and continues to be an important property characterizing color centers. While the present work has reported decay

temperatures for both the V_K and V_{KA} centers, these temperatures were obtained utilizing different experimental techniques, pulsed anneal (V_{KA}) vs. continuous warming (V_K). Improved experimental capabilities would allow a pulse anneal study of the V_K center.

Motional effects for the V_{KA} center were reported; however, only over a limited temperature range. The study should be extended over a larger temperature interval and expanded to include the V_K center. Existing dewar systems did not allow a large temperature variation about the fixed nitrogen and helium temperature points. The flexibility offered by a gas exchange system would permit continuous temperature variations between 5 and 77K.

Previous radiation damage studies in MgF_2 have revealed three intriguing effects which, with further study, could possibly be related to the present investigation. These are:

1. The inability to damage MgF_2 near 150K.
2. The sharp thermal anneal stages of F centers at 70 and 150K and
3. The possibility of the F-H center close pairs.

Important questions such as "Is there any correlation between the first stage F center decay at approximately 70K and the presently determined 60-65K anneal of the V_K center? Is the resistance to damage at 150K related to motional effects or the lack of stabilization sites for interstitials? Do the back reactions during irradiation, coupled with the lack of electron traps, completely eliminate stabilization of the interstitial H center?" As these questions indicate, additional work is needed before a complete understanding of radiation damage in MgF_2 is obtained.

BIBLIOGRAPHY

1. Sonder, E., and W. A. Sibley, "Defect Creation by Radiation in Polar Crystals." Point Defects in Solids, Volume I, General and Ionic Crystals. J. H. Crawford, Jr. and L. M. Slifkin, eds. New York: Plenum Press, 1972, pp. 201-283.

2. Abragam, A., and B. Bleany. Electron Paramagnetic Resonance of Transition Ions. Oxford: Clarendon Press, 1970.

3. Feher, G., Phys. Rev. 114, 1219 (1959).

4. Crawford, J. H., Jr., Adv. in Phys. 17, 93 (1968).

5. Fowler, W. B., in Physics of Color Centers, W. B. Fowler, ed., Academic Press, New York, 1968.

6. Seitz, F., Phys. Rev. 79, 529 (1950); Rev. Mod. Phys. 26, 7 (1954).

7. Varley, J. H. O., Nature, Lond. 174, 886 (1954a).

8. Howard, R. E. and R. Smoluchowski, Phys. Rev. 116, 314 (1959).

9. Dexter, D. L., Phys. Rev. 93, 985 (1954); Ibid., 118, 934 (1960).

10. Itoh, N., J. Sharma, and R. Smoluchowski. 1965, International Symp. on Color Centers in Alkali Halides, Urbana, Ill., Abstract No. 95.

11. Klick, C. C., Phys. Rev. 120, 670 (1960).

12. Howard, R. E., S. Vosko, and R. Smoluchowski, Phys. Rev. 122, 1406 (1961).

13. Balarin, M., Kernenergie 7, 434 (1964).

14. Hall, T. P. P., D. Pooley, and P. T. Wedepohl, Proc. Phys. Soc. 83, 635 (1964).

15. Konitzer, J. D. and H. N. Hersh, J. Phys. Chem. Solids 27, 771 (1966).

16. Hersh, H. N., Phys. Rev. 148, 928 (1966).

17. Pooley, D., Proc. Phys. Soc. 87, 245 (1966).

18. Pooley, D., Proc. Phys. Soc. 87, 257 (1966).

19. Kabler, M. N., Phys. Rev. 136, A1296 (1964).

20. Murray, R. B. and F. J. Keller, Phys. Rev. 137, A942 (1965).

21. Murray, R. B. and F. J. Keller, Phys. Rev. 153, 993 (1967).

22. Lushchik, C. B., G. K. Vale, E. R. Ilmes, N. S. Rooze, A. A. Elango, and M. A. Elango, Optics and Spectra. 21, 377 (1966).

23. Itoh, N. and M. Saidoh, J. de Physique 34, (Supplements) 101 (1973).

24. Castner, T. G. and W. Känzig, J. Phys. Chem. Solids 3, 178 (1957).

25. Daly, D. F. and R. L. Mieher, Phys. Rev. Letters 19, 637 (1967); Phys. Rev. 175, 412 (1968).

26. Delbecq, C. J., B. Smaller, and P. H. Yuster, Phys. Rev. 111, 1235 (1958).

27. Delbecq, C. J., W. Hayes, and P. H. Yuster, Phys. Rev. 121, 1043 (1961).

28. Keller, F. J. and R. B. Murray, Phys. Rev. Letters 15, 198 (1965); Phys. Rev. 150, 670 (1966).

29. Riley, C. R. and W. A. Sibley, Phys. Rev. B1, 2789 (1970).

30. Känzig, W., J. Phys. Chem. Solids 17, 80 (1960).

31. Känzig, W. and T. O. Woodruff, J. Phys. Chem. Solids 9, 70 (1958).

32. Delbecq, C. J., J. L. Kolopus, E. L. Yasaitis, and P. H. Yuster, Phys. Rev. 154, 866 (1967).

33. Keller, F. J. and F. W. Patten, Solid State Commun. 7, 1603 (1969).

34. Wertz, J. E. and J. R. Bolton, Electron Spin Resonance: Elementary Theory and Practical Applications. New York: McGraw-Hill Book Company, 1973.

35. Abragam, A. and B. Bleaney, Electron Paramagnetic Resonance of Transition Ions. Oxford: Clarendon Press, 1970.

36. Orton, J. W., Electron Paramagnetic Resonance. An Introduction to Transition Group Ions in Crystals: London Iliffe Books LTP, 1968.

37. Bleaney, B. and K. W. H. Stevens, Rept. Prog. Phys. 16, 108 (1953).

38. Bowers, K. P. and J. Owen, Rept. Prog. Phys. 18, 304 (1955).

39. Jarrett, H. S., in Solid State Phys. Vol. 14; Editors: F. Seitz and D. Turnbull, Academic Press (1963).

40. Anderson, E. E., Modern Physics and Quantum Mechanics. W. B. Saunders Company. 1971, p. 289-332.

41. Poole, C. P. and H. A. Farach, The Theory of Magnetic Resonances, John Wiley and Sons (1972), p. 82-101.

42. Farach, H. A. and C. P. Poole, Adv. Magnetic Resonance 5, 229 (1971).

43. Megaw, H. D., Crystal Structures: A Working Approach. W. B. Saunders Co., Philadelphia, p. 257-258 (1973).

44. Duncanson, A. and R. W. H. Stevenson, Proc. Phys. Soc. (London) 72, 1001 (1958).

45. Hills, M. E. and W. R. McBride, J. Chem. Phys. 40, 2053 (1964).

46. Blunt, R. F. and M. I. Cohen, Phys. Rev. 153, 1031 (1967).

47. Sibley, W. A. and O. E. Facey, Phys. Rev. 174, 1076 (1968).

48. Sibley, W. A., IEEE Transactions on Nuclear Sciences 18, Dec. (1971) p. 273.

49. Facey, O. E., D. L. Lewis, and W. A. Sibley, Phys. Stat. Sol. 32, 831 (1969).

50. Unruh, W. P., L. G. Nelson, J. T. Lewis, and J. L. Kolopus, J. Phys. C: Solid State Phys. 4, 2992 (1971); Ibid., J. Phys. C: Solid State Phys. 4, 3007 (1971).

51. Buckton, M. R. and D. Pooley, J. Phys. C: Solid State Phys. 5, 1553 (1973).

52. Rhoads, J. E., Dissertation presented to Oklahoma State University Graduate College, Stillwater, Oklahoma (p. 18-28), 1972.

53. Little, E. P., Thesis presented to Oklahoma State University Graduate College, Stillwater, Oklahoma (p. 9), 1976.

54. Riley, C. R. and W. A. Sibley, Phys. Rev. B1, 2789 (1970).

55. Schoemaker, D., Phys. Rev. B7, 786 (1973).

56. Pryce, M. H. L., Proc. Phys. Soc. (London) A63, 25 (1956).

57. Hall, T. P. P., Brit. J. Appl. Phys. 17, 1011 (1966).

58. Bailey, C. E., Phys. Rev. 136, A1311 (1964).

59. Bass, I. L. and R. L. Mieher, Phys. Rev. 175, 431 (1968).

60. Lewis, J. T., J. L. Kolopus, E. Sonder, and M. M. Abraham, Phys. Rev. B7, 810 (1973).

61. Chase, L. L. and H. J. Guggenheim, Physics Letters 28A, 694 (1969).

62. Zaripov, M. M., V. S. Kropotov, L. P. Livanova, A. L. Stolov, and Zh. S. Yakovleva, Soviet Physics--Solid State 8, 2948 (1967), Translated from Fizika Tverdogo Tela, Vol. 8, No. 12, pp. 3680-3681, December, 1966.

63. Zaripov, M. M., V. S. Kropotov, and L. D. Livanova, Soviet Physics--Solid State 8, 81 (1966), Translated from Fizika Tverdogo Tela, Vol. 8, No. 1, pp. 231-233, January, 1966.

64. Sturge, M. D., F. R. Merritt, L. F. Johnson, H. J. Guggenheim, and J. P. Van Der Z el, J. of Chem. Physics 54, 405 (1971).

65. Gerritsen, H. J., S. E. Harrison, H. R. Lewis, and J. P. Wittre, Phys. Rev. Letters 2, 153 (1959).

VITA

Claude Donald Norman

Candidate for the Degree of

Doctor of Philosophy

Thesis: RADIATION DAMAGE IN MAGNESIUM FLUORIDE

Major Field: Physics

Biographical:

Personal Data: Born in Lincoln County, Georgia, July 17, 1936, the son of Claude and L. E. Norman.

Education: Attended primary and secondary schools in Elberton, Georgia; graduate from Elberton High School in 1954; received the B.S. degree from Berry College, Mt. Berry, Georgia in June 1958; received the Master of Science degree in physics from University of Georgia, Athens, Georgia, in 1967; attended Oklahoma State University, Stillwater, Oklahoma, 1974-1976; completed requirements for the Doctor of Philosophy degree in July, 1976.

Experience: Employed as teaching and research assistant in the Physics Department of the University of Georgia (1958-1965); Research Associate at Oak Ridge Associated Universities (1965-68); Assistant Professor of Physics, Georgia Southwestern College, Americus, Georgia (1969-74); Teaching and research assistant, Oklahoma State University, Stillwater, Oklahoma, 1974-1976.